Shear Strength Deterioration Effect and Slope Reliability Analysis Under Extreme Ice-snow Melting Conditions

Tongqiang Xiong (scixiong@126.com)
China Three Gorges University
Jianlin Li
China Three Gorges University
Lehua Wang
China Three Gorges University
Huafeng Deng
China Three Gorges University
Xiaoliang Xu
China Three Gorges University

Research Article

Keywords: ice-snow melting, deterioration effect, physical process, matric suction, creep model, copula

Posted Date: March 11th, 2021

DOI: https://doi.org/10.21203/rs.3.rs-263468/v1

Shear strength deterioration effect and slope reliability analysis under extreme ice-snow melting conditions

Tongqiang Xiong[1,2,*], Jianlin Li[1,*] ,Lehua Wang[1],Huafeng Deng[1],Xiaoliang Xu[1]

[1] **Key Laboratory of Geological Hazards on Three Gorges Reservoir Area of Ministry of Education, China Three Gorges University, Yichang City 443002, Hubei Province, China**

[2] **College of Hydraulic & Environmental Engineering, China Three Gorges University, Yichang 443002, Hubei, China**

***Corresponding. scixiong@126.com, ljl@ctgu.edu.cn.**

ABSTRACT

Extreme ice-snow melting in winter affects the infiltration process of snow water on the slope surface significantly, and plays an important role in the deformation stability of landslide. The fluctuation trend of slope stability under ice-snow melting is the same as that of soil volume water content. The deterioration effect of mechanical parameters will directly affect the deformation stability of bank slope. Based on this, the ice-snow melting cycle model test of slope soil was designed and carried out. The results are showed.(1) We were established an ice-snow melting model based on physical process. In the process of ice-snow melting, the soil cohesion and internal friction Angle have obvious deterioration effect .The deterioration of cohesion is obviously larger than that of internal friction Angle. In the early part of the ice-snow melting cycle, the deterioration of shear strength parameters is very obvious. Among them, the deterioration of shear strength parameters caused by the first four ice-snow melting cycles accounted for about 70% of the total deterioration. After the G2/T2 ice-snow melting cycle, the degree of phase deterioration gradually decreases. The deterioration trend of shear parameters of soil samples gradually tends to be gentle. (2) In the ice-snow melting cycle, the inside of the soil samples have micro-cracks, fissures repeatedly opened and closed, gradually developed and converged. The result is that the soil samples change from dense state to loose state where internal cracks develop. The internal damage of soil samples is the fundamental reason for the gradual deterioration of shear strength.（3）We are keep to the relative independence principle of creep model and unsaturated seepage equation. We are studied and improved the parameter solving method of creep model. The modified model is reasonable and effective. The creep trend and main characteristics of the unsaturated soil can be described well. Shear strength deterioration effect and slope reliability analysis under extreme ice-snow melting conditions .It has important reference significance to the protection of extreme snow and ice disaster on the bank slope.

KEYWOEDS: ice-snow melting; deterioration effect; physical process; matric suction; creep model; copula

---

Introduction

The rapid huge landslide occurred in Yi gong River in the Bo mi, Tibet, on the April 9, 2000[1]. The Yi gong Landslide is caused by the melting of snow and ice on Xuefeng mountain, resulting in the formation of debris flow, which was a huge disaster[2].Geological disasters caused by melting ice and snow are common. The volume of the Alps is larger than that of the Swiss Alps $10^8 m^3$.There are dozens of extremely large landslides [3]. Most of them are caused by rock mass loosening and water saturation caused by the melting of ice and snow during the retreat of Quaternary glaciers[4].A large number of landslides occurred in Japan from February to March 2006 due to the melting of ice and snow[5-8]. The extreme ice snow disaster climate rarity appears in the Three Gorges Reservoir Area, the probability is very small. The geological disaster caused by it has not been paid enough attention it [9,10]. There is a great difference with the alpine region， in the topography, geological environment, climate environment. In early 2008, the rare ice-snow climate occurred and induced large geological disasters in southern China[11-13].One high loess slopes, which was located in Yi li Region of Xinjiang ， reactivated and

caused long-distance road burying and river blocking on April 30，2019[14]. The rapid snow ablation and infiltration drive by the abnormal temperature rising in spring was the most important influencing factor on deformation evolution of the loess slope[15]， and the coupling of thawing water and rainstorm in spring was the fundamental reason controlling the occurrence of loess landslides[16]. A large number of soil slope are instability occurred after the peak of ice-snow melting, indicating that there is a very close relationship between soil slope instability and ice-snow melting [17]. The ice-snow melting infiltration were greatly reduces the shear strength of soil, and collapsible deformation occurs under the softening action of water. With the change of its hydrologic properties, the mechanical strength will greatly decrease, which is an important factor inducing soil landslide [18-24]. The cohesion and internal friction angle of soil were show different variation rules under different condition[26,27]. The main reason of soil slope is shown instability caused as follows, there have two facts. On the one hand, ice-snow melting is leads to the disappearance of matrix suction in soil .On the other hand , the temporary of pore water pressure will increase in the transient saturated zone[28].From the perspective of effective stress, under the condition of the increase of pore water pressure, the decrease of effective stress in the soil body of the slope is the main reason for the decrease of shear strength of soil [29].From the perspective of effective stress, the increase of pore water pressure and the decrease of effective stress are the main reasons for the decrease of soil shear strength.

On the basis of laboratory tests, a large number of creep models have been established by predecessors through theoretical analysis[30,31]. In terms of creep characteristics of saturated soil, a multi-dimensional logarithmic functional model is describing strain time relationship in uniaxial compression creep test[32,33]. Hyperbolic model or power function model is generally used to describe the strain time relationship in the triaxial creep tests. Experimental study of creep characteristics under different water content, one-dimensional consolidation and the triaxial compression tests were carried out on saturated, wet, air-dried and dried clays [34].It is pointed out that the viscosity coefficient of saturated sample is higher than that of unsaturated sample. Many scholars were carried out the uniaxial compression and the triaxial creep tests of mudstone with different water content[35]. The results have shown the uniaxial compression strength and elastic modulus of mudstone samples decrease significantly with the increase of water content, and the creep strain rate increases with the increase of water content [36-37].

Snow melt model is a tool to quantitatively describe the process of snow melt. It is closely related to the development of snowmelt runoff hydrological model[44,45]. Snowmelt models are included single point model and spatial distributed model[46]. We are integrated Hydrological Confluence Module. The single point melt water process is converged to the section to calculate. The single point snowmelt model is coupled to the snow scheme in GCM to realize the snow cover calculation[47]. According to different melt water algorithms, snow melt models can be divided into temperature index method and energy balance method[48]. According to the temperature index method, there is a certain correlation between snow melt amount and temperature.

The bank slopes are covered by extreme ice and snow. There are many uncertainties in the stability of bank slope. Geotechnical parameters are often difficult to obtain, especially in situ parameters. The small sample problem is arises. They [49] had proposed a small sample expansion method based on Bootstrap. According to this, we are try to determine the optimal edge distribution function of the variable and the optimal Copula function recognition method. They [50-52] also discussed the system reliability of geotechnical structures (such as retaining walls) with the help of Copula function. They[54]had analyzed the shear strength parameters of rock mass and their correlation with Q value of rock mass and deformation parameters with the help of Copula function. Try to predict some parameters that are hard to measure, such as the elastic modulus of rock mass. They[55]had established the joint distribution model of landslide scale, occurrence frequency and stable state with the help of Copula function. Copula is successfully applied to regional landslide disaster assessment using conditional probability theory.

At present, there are few experimental studies on extreme ice-snow melting in the Three Gorges Reservoir area. We are discussed the deterioration effect of bank slope soil under ice-snow melting. The deterioration of physical and mechanical properties of soil mass during ice-snow melting action is a gradual and long-term process. The macro phenomenon in the short term is local bank collapse or small scale deformation and failure. However, the cumulative damage effect cannot be ignored for the overall deformation and stability of the bank slope.

Material and methods

Study on ice-snow melting model

We are chooses a homogeneous slope in the Three Gorges reservoir area as the research object. In accordance with the "Geotechnical Test Procedure" [21], we have tested and analyzed the basic physical and mechanical parameters of the unmodified soil samples retrieved from the site. The mechanical parameters of the material are as follows: Elastic modulus E is 2.6MPa,Poisson's ratio μ is 0.31, cohesion c is 14kPa, angle of internal friction φ is 19o,γ is 19.7kN/m^3,Saturation permeability coefficient Ks is 2.28*10^{-6} (m/s). Natural moisture content is 17.92%.The parameters are shown in table 1. Grading curves of soil sample is shown in Figure 1.P≤0.075 mm is 85.963%,P≤0.075mm is represents the percentage of cumulative mass of particles with particle size no more than 0.075mm in total mass. Where，% is the mass percentage of soil less than a particle size.

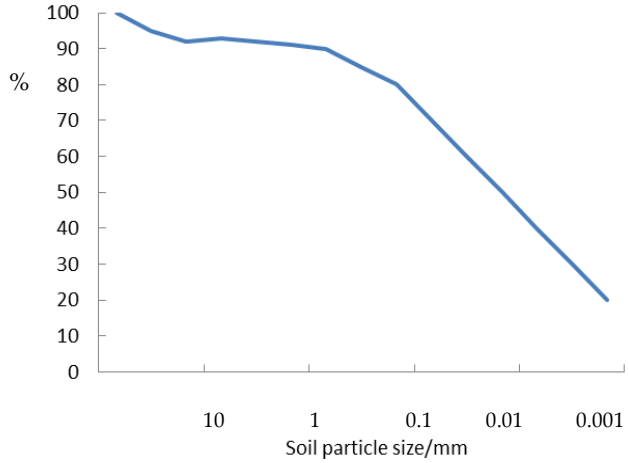

Figure 1. Grading curves of soil sample

$\gamma(kN/m^3)$	Ks(m/s)	C(kPa)	φ	E(MPa)	μ
18	2.28*10^{-6}	19.3	18.5°	2.6	0.31

Table 1. The basic property of soils

In this experiment, two small scale (2mx1mx1.5m) glass tanks of the same size were prepared to carry out the ice-snow melting model test.

In this experiment, we were carried out total of 6 times ice-snow melting model tests. There are two groups with three times in each group. One time test lasted 24 hours, and three times lasted 96 hours. Each test tank was evenly covered with snow 30cm at a time. The results of many tests are show as follow. The multi-stage model test of ice-snow melting is shown in Figure 2.

(**a**) Matrix suction sensor (**b**)Data logger

(**c**) Model snow whole picture (**d**) Model snow positive

(**e**) moisture sensor (**f**) Field test

Figure2. Multi-stage model test of ice-snow melting

We are take 30° slope foot as an example. We are layout three moisture content sensors and three matrix suction sensors .As shown in Figure 3.

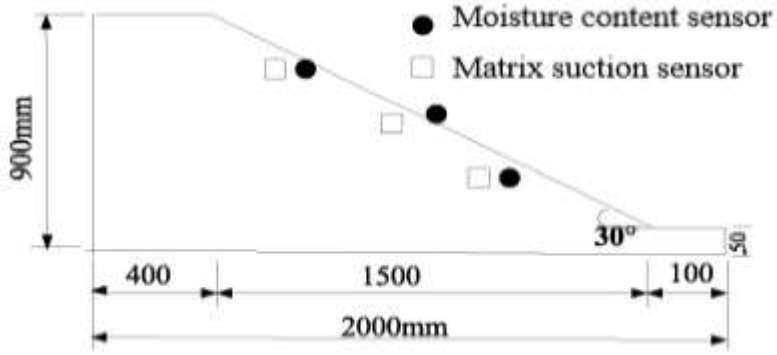

Figure 3. Sensor layout (take 30° slope foot as an example)

We have routinely two kind observation snowfall. There are from meteorological and hydrological services department 13. One is the depth of snow in centimeters; the other is snow equivalent, which is the depth of snow into a layer of water-the amount of rainfall, measured in millimeters. In this test, the amount of snow 30cm thick was laid, and the ambient temperature and snowmelt rate were controlled during the test. The experimental scheme and part of the measured data are shown in Table 2.

G/ T	h	α	v	t	w	s
	cm	°	cm/h	h	%	kPa
G1/T1	90	30°	1.25	24	33	-10
G1/T2	120	45°	1.5	20	35	-50
G1/T3	120	60°	2	15	48	-150
G2/T1	90	30°	3	10	45	-100
G2/T2	120	45°	4	7.5	50	-200
G2/T3	120	60°	5	6	52	-300

Table 2. Experimental scheme and part of the measured data

In table 2, G/ T is test Group/Time of ice-snow melting, h is refers height of the model slope, α is refers to the model angle at the foot of the slope, v is refers to the melting rate of ice and snow, t is the melting time of ice and snow, w is the percentage moisture content, s is refers to the matric suction sensor.

Ring knife collect samples

The ice-snow was completely melted on the slope surface. We are used a ring cutter to sample the slope toe surface at 10cm intervals along the broken face The two groups have six ice-snow melting tests, 30min after thawing of each test bank slope surface. During the initial sampling, the soil sample is closely attached to the inner wall of the ring knife, and the height is flush with the upper surface of the ring knife. We are used a ring cutter to sampled 20cm from the foot of the slope. Make 5 samples and 1 spare sample for each time. As shown in Figure 4.

(a)Ring knife collect samples (b) Direct shear instrument

Figure 4. Direct shear test of soil samples

Test results and analysis

Deterioration law of shear strength of soil

Routine indoor shear tests were conducted on the above ring knife soil samples, and analyzed the soil degradation effect. In the process of snowmelt infiltration, the soil water content was increased gradually, the soil bulk density was increased, and the matric suction was decreased. There are led to the decrease of the soil shear strength. Snowmelt infiltration is a continuous dynamic process, Slope failure is usually occurs during the peak period of continuous snowmelt or sometime after the snowmelt stops. The ice-snow melting is seeps through cracks in the ground. It is gradually moistens and softens. The shear strength is greatly reduced. As the cracks expand and the water seeps, it will change the water flow conditions in the slope. The softening range of soil in the saturated area of the slope is further expanded.

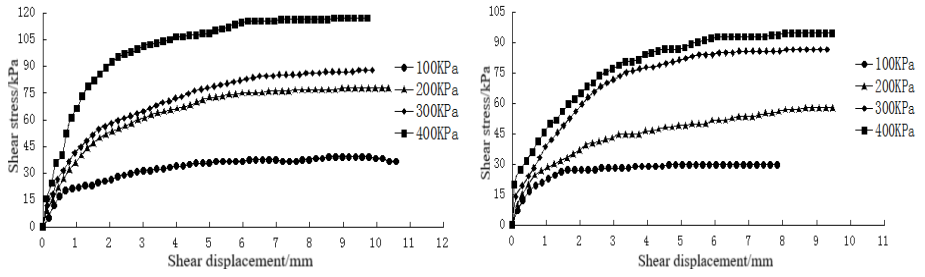

(a)Ice-snow melting G1/T1 (b)Ice-snow meltingG1/T3

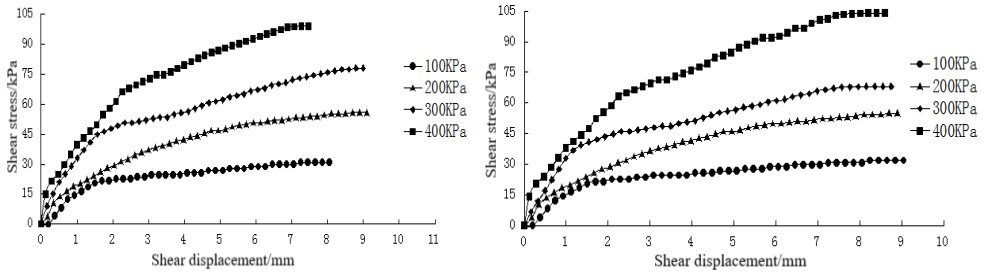

(c)Ice-snow melting G2/T2 (d)Ice-snow melting G2/T3

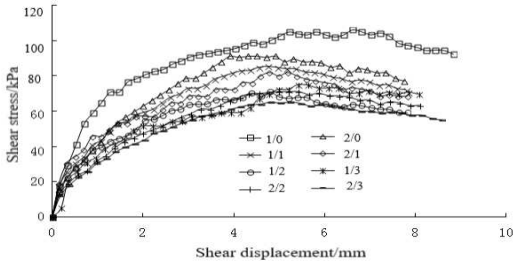

(e) Normal stress 400kPa

Figure 5. Ice-snow melting shear stress and shear displacement curve

The Figure 5 was shows specimens of different ice-snow melting Groups/Time show similar deformation characteristics in stress-strain. Under the same normal stress state, the slope of the initial loading stage and shear strength are gradually decreases, with the increase of ice-snow melting times. That is, the stress is increases rapidly in the early stage and slows down in the later stage. The slope of the curve is continuously changes from larger to smaller. The results are indicated the shear strength of soil samples gradually deteriorates due to the ice-snow melting. There has peak intensity, but it was not particularly significant. The peak strength is increases with the increase of vertical stress.

G/ T	c	$(t\text{-}d)_c$	$(s\text{-}d)_c$	φ	$(t\text{-}d)_\varphi$	$(s\text{-}d)_\varphi$
	kPa	%	%	°	%	%
G1/T0	18.51			19.29		
G1/T1	15.62	15	15	18.31	5.08	5.08
G2/T1	13.23	28	13	17.65	8.55	3.48
G1/T2	10.25	45	17	16.79	13.12	4.56
G1/T3	9.73	52	8	16.38	15.23	2.03
G2/T2	7.85	57	2.4	15.73	18.48	2.07
G2/T3	7.5	60	2.4	15.52	19.93	1.45

Table 3. Shear strength degradation parameters in ice-snow melting.

We are use the Moor-Coulomb rule. We are according to the fitting analysis of direct shear test results of soil samples under different normal stresses in the ice-snow melting process. We are obtained the cohesion and internal friction Angle of soil samples under ice-snow melting through experiments. This is shown in Table 3. Where, $(t\text{-}d)_c$ and $(t\text{-}d)_\varphi$ are c and φ total degradation ; $(s\text{-}d)_c$ and $(s\text{-}d)_\varphi$ are c and φ stage degradation.

We are compared analyzing the test results. The deterioration degree of ice-snow melting is defined reduction degree of shear strength parameter. Where, Si is the total deterioration degree. ΔS_i is shear strength parameters of the degradation degree of single time ice - snow melting. Si and Δ Si computation formula is as follows.

$$S_i = (T_0 - T_i) / T_0 \times 100\% \quad (1)$$

$$\Delta S_i = S_i - S_{i-1} \quad (2)$$

Where, T_0 is the shear strength parameter of the soil sample in the initial state of water saturation, including cohesion C and internal friction Angle φ. T_i is the shear strength parameter value of different times of snow melting in the ice-snow melting process. The total and the phase deterioration curves of cohesion and internal friction Angle are listed in Figure 6 and Figure 7. Combining the two figures, it can be seen that:

(1) In the case of ice-snow melting, the cohesion and the deterioration of internal friction Angle are generally consistent. However, the deterioration of cohesion is obviously larger than the internal friction Angle. After G1/T1 ice-snow melting, the cohesion and internal friction Angle are respectively decreased by 15% and 5.08%, respectively. After G1/T3 ice-snow melting, the cohesion and internal friction Angle are respectively decreased by 52% and 15.23%.After G2/T3 ice-snow melting, the cohesion and internal friction Angle are respectively decreased by 60% and 19.93%.

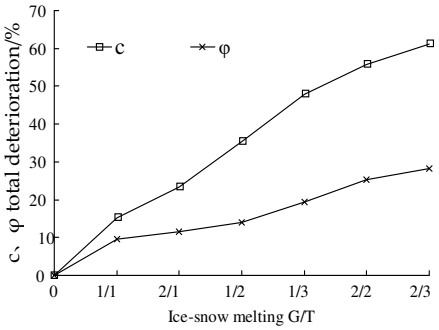

198

199 **Figure 6.** Total deterioration degree curves of cohesive force and internal friction angle

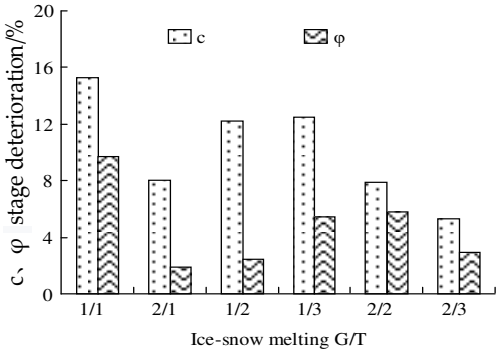

200

201 **Figure 7.** Stage deterioration degree curves of cohesive force and internal friction angle
202
203 (2) Under the action of ice-snow melting cycle, the deterioration effect of shear strength parameters has
204 obvious non-uniformity. The shear strength parameters are deteriorated significantly, there are due to the
205 previous four ice-snow melting cycles. The degree of phase deterioration is obviously larger. It's about 70% of
206 the total deterioration. After the G2/T2 ice-snow melting cycle, the stage deterioration are gradually decreased.
207 The deterioration trend of shear parameters is gradually gentle.
208 (3)Assume that the damage to soil samples is a continuous process. We are established the damage evolution
209 equation of soil shear strength parameters. The deterioration trend of shear strength parameters of soil samples
210 can be well fitted by logarithmic function. The fitting curve is shown in Figure 8.

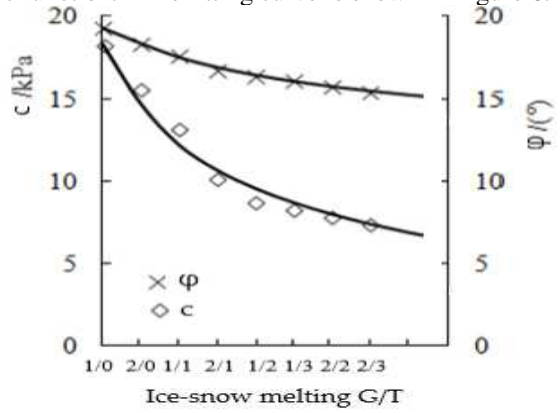

211
212 **Figure 8.** Deterioration rules of cohesive force and internal friction angle in ice-snow melting
213
214 Where, n is the number of times that the bank slope encounters ice-snow melting. The deterioration equations
215 are shown in the equation (3) and (4).

$$c = 19.29[1 - 0.09\ln(1+6.453n^{2.157})] \quad (3)$$

$$\varphi = 18.5l[1 - 0.06\ln(1+1.167n^{1.615})] \quad (4)$$

Deterioration mechanism of soil physical properties in ice-snow melting

During the ice-snow melting process of soil, water molecules are repeatedly infiltrate and outside the soil body. There are water molecules infiltrate, physical and chemical interactions and ion exchange occur between water and soil minerals. The mineral particles themselves and the cements are softened, the bonding force is weakened and the molecular attraction is reduced. With the increase of porosity in the soil sample, the volume expansion is presented macroscopically, and the corresponding shear strength decreases. During the drying process, water molecules are seep out, and the strength of mineral particles and cements is partially restored. But it's not a completely reversible process. At the same time, in the process of soil sample drying, the water molecules are uneven loss from the inside to the outside and the uneven structure of soil sample. There are many micro and macro cracks in the soil sample. The existence of these cracks are provides more channels and more space for the physical, chemical and ion exchange of the next ice melt.

Figure 9. Crack growth of sample surface

In the process of ice-snow melting, the soil samples are repeatedly swelling with water absorption and shrinking with water loss. The pores in the soil samples are gradually increase, the micro-cracks and cracks gradually open, expand, converge and connect. The structural integrity of soil is gradually destroyed. This point can also be well confirmed by the crack development law on the surface of the soil sample in Figure 9. Therefore, the ice-snow melting process is a cumulative damage process for the internal structure of soil samples. It's a process of influence from micro to macro. Thus, the shear strength of soil are deteriorates. After many times ice-snow melting, the damage process of the internal structure of the soil sample are gradually tends to be slow under the action of the lateral restriction of the ring knife. The deterioration trend of shear strength parameters is also gradually slow.

The cohesion of soil are mainly comes from the bonding force and molecular attraction mineral grains, mineral particles formed cement bonding force between particles and the surface tension of additional adsorption force between [38-40].The Ice-snow melting is leads to the full development of internal structural damage of soil samples. The mineral particles themselves soften with the cements. The bonding force and molecular attraction are weakened. Therefore, the cohesion is deteriorates significantly faster. The effective internal friction angle of soil is less affected by external force and suction. Mainly depends on its mineral composition and stress history [41]. The mineral particles are softening during ice-snow melting. The soil structures are damage and deterioration of during ice-snow melting. This is results in the decrease of the internal friction Angle of the soil sample. But the decline was relatively small.

Ice-snow melting process model

Model structure

Physical model test is an important method to study ice-snow melting. The calculation methods have mainly included temperature index method and energy balance method. The temperature index method is a certain correlation between snow melt and temperature. The deformation of snow water infiltration line is shown in

Figure 10. The infiltration boundary condition is controlled by snowmelt intensity. The depth of wetting front is increases linearly with the duration of snowmelt. The boundary is controlled by soil infiltration capacity in the late period of snowmelt. The infiltration rate is gradually decreased eventually stabilizes. The depth of wetting front is nonlinear with snowmelt time.

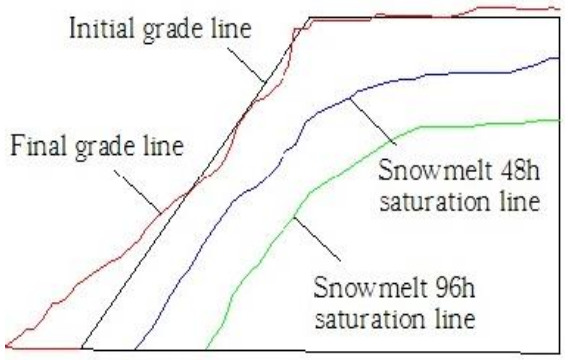

Figure 10. Infiltration line of snow water

When melting conditions are met, the snow begins to melt. It is important to estimate the intensity or rate of snow melt and the amount of snow melt over a period of time. The intensity and amount of snow melt are determined by the condition of snow cover and the heat balance condition of snow melt. We are calculate the amount snow of evaporate and sublimate based on latent heat flux. The latent heat flux have two step action .Firstly, it is satisfies the evaporation of liquid water on the surface. Secondly, it is sublimates the solid ice on the surface. And so on, step by step down.

We are aim to build point-scale models of snowmelt based on physical processes. Firstly, the point-scale model can be directly verified by observation data. Secondly, point-scale model is the base and core algorithm of spatial distribution snowmelt model. Thereafter, the spatiotemporal distributed model can be built gradually by coupling the integration technology with the dynamic confluence module.

The model are includes four main parts.

(1)The energy balance;

(2)The phase change (The mass conservation);

(3)Water balance;

(4) The particle size change and compaction.

The whole snow cover is divided into n layers with a certain space step △Z. Each layer are contains three phases: solid, liquid and gas, respectively denoted by subscript i, w and a.

Energy balance

In this paper, snow water equivalent is expressed by snow depth (m) × density (kg/m 3).In the simulation, the snow equivalent decreases, the snow cover becomes thinner, and the density increases, but the product goes down. After the snow cover absorbs energy. On the one hand, it is reflected by the overall melting of the snow layer, the thickness of the snow thinning and the outflow of the snow melt. On the other hand, the partial melting of snow layer, the loading compaction of the negative snow layer and the increase of the density of this layer. At the initial stage of ablation, the incident energy was large, the whole layer ablation was dominant, and the thickness of snow cover decreased significantly. When the incident energy is small, the compaction and density are increase of the snow cover by partial ablation significant. At the later stage of ablation, snow thickness decreased and density increased with the increase of radiation. With the input of energy, the increase of snow cover density changes non-linearly.

The energy balance model,

$$c_s \rho_s \frac{\partial T}{\partial t} = \lambda_s \frac{\partial^2 T_s}{\partial z^2} + \mu S_{net} \exp(-\mu z) - M \tag{5}$$

The upper boundary conditions for heat flux control[43],

$$c_s \rho_s \frac{\partial T}{\partial t}.dz = \lambda_s (\frac{\partial T}{\partial z})\Big|_{z=0} + (\mu S_{net} \exp(-\mu z) - M)dz + L_{in} - L_{out} + H - lE \quad (6)$$

S_{net} is the net shortwave radiation (Lin-Lout)， W/m^2; λ_s is snow heat conductivity，W/m·℃; c_s is the specific heat of the snow layer，J/kg·℃; M is the ice-snow melting speed ， kg/s; μ is the attenuation coefficient of solar radiation in the snow layer. Recommended value is 40 m^{-1}.

Phase change process

In this paper, the dynamic melting of snow cover and the change of soil moisture were studied by increasing ambient temperature in the control test method. The purpose was to understand the law of the melting and the change characteristics of soil moistures content, under the condition of increasing temperature in the snowmelt period.

The energy balance equation can calculated the temperature profile of the snow layer. The actual temperature of the snow layer is Ts (Z, t) ≤0 ℃. There is a calculation of snow temperature Ts>0℃. Firstly, it is assumed that the critical temperature of snowmelt Tm is 0℃. Secondly, it is reset the temperature of the snow layer to 0.Finally, surplus energy is used for heating and melting model calculation.

$$\Delta m_w = \Delta(SWE \times \varphi_w) = c_i m_i (T_s' - T_m) / L_f \quad (7)$$

The liquid water is transferred between the snow layers according to the infiltration rate, and the maximum liquid water content of the snow layer is the upper limit, and the remaining water continues are transfer to the lower layer.

$$\frac{\partial WC}{\partial t} = K_w \quad (\varphi_w \le \varphi_{w\_max}) \quad (8)$$

Where, WC is water transfer between snow layers， kg; Kw is infiltration rate, kg / s; φ_{w_max} is the maximum mass content of liquid water in snow layer.

$$Kw = K_s . S_e^a = K_s[(\theta - \theta_i) / (n - \theta_i)]^a \quad (9)$$

$$K_s = 0.08 d^2 \exp[-0.008(\rho_i / \rho_w)] \quad (10)$$

Where， θ is liquid water content; θ_i is Capillary water content; n is porosity; S_e is saturated moisture content; K_s is saturation conductivity, kg/s; d is snow particle size, m; a is parameter， the recommended values is 2. 8.

Along with the melting transfer process, the possible conditions are described below.

(1) The snow layer are becomes thinner and the density decreases;

(2) The snow layer is gradually melting;

(3) When the density is lower than a critical value ρ_{min}, the snow layer collapses and melts completely.

Creep model of unsaturated soil under ice-snow melting

The matric suction of unsaturated soil was varies with the water content. Thus, the shear strength index was changes. Slope stability is affected. Many times artificial snow are paving in the slope. The water holding capacity is affected by the humidity. The water holding capacity is decrease with the increase the number of ice-snow melting. The compressibility was same as decrease by the porosity. Water holding capacity and compressibility of soil under different consolidation pressures are shown in Figure 11.

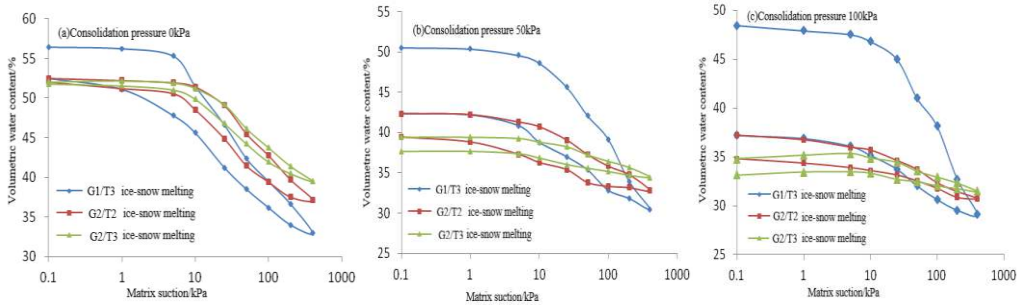

Figure 11. Relationship between water holding capacity and compressibility

We are carried out uniaxial compression and triaxial creep tests under different water content. The results are show that the compressive strength and elastic modulus are decrease significantly with the increase of water

content. The strain rate is increases with the water content. The water holding capacity of soil was decreases by the increase of ice-snow melting. The porosity was decreases, same as compressibility. The soil water holding capacity under the action of multiple ice snow melting is affected by the increase and decrease of humidity, as shown in Figure 12.

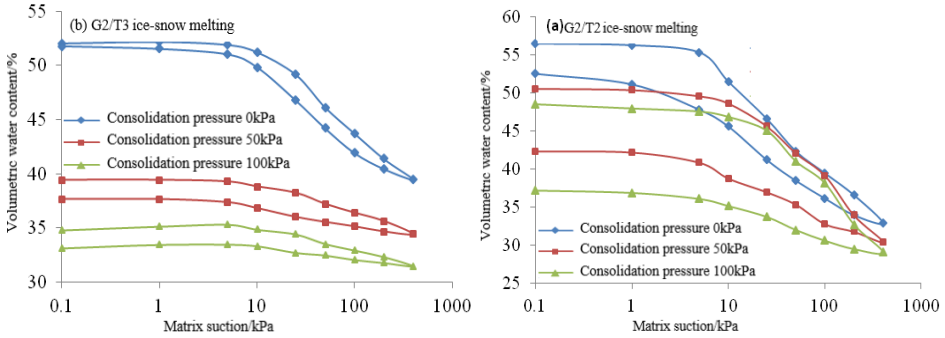

Figure12. Effect of soil moisture and water holding capacity

The water holding characteristics of ice-snow melting are satisfied the hysteresis loop characteristics. There are shown in figure.5 and figure.6. With the same ice-snow melting intensity, the matric suction is gradually decreases at each measuring point of the slope, as the flow of snow water infiltration increases. The matric suction is rapidly decreased in the first 12h at each measuring point along the flow. And, it is slowly in the last 12h.

In the same section, the matric suction is rapidly decreases in the later period. Among, the foot of slope is more drastic change. With the increase of the depth of the measuring point, the matric suction was gradually weakened. The shear strength of unsaturated soil was increases with the increase by matric suction, but the rate is gradually decreases.

Based on the soil-water characteristic curve (SWCC), it can be seen that the infiltration process of ice -snow melting is essentially of soil moisture absorption. With the increase of soil porosity n, the creep model is established which can quantitatively reflect the long-term deformation of unsaturated soil. Creep test curve for controlling matric suction is shown in Figure 13. We are established the stress-suction-strain-time model of the test soil. The modified model can reasonably describe the rapid decay creep of soil in the initial stage and the stable creep.

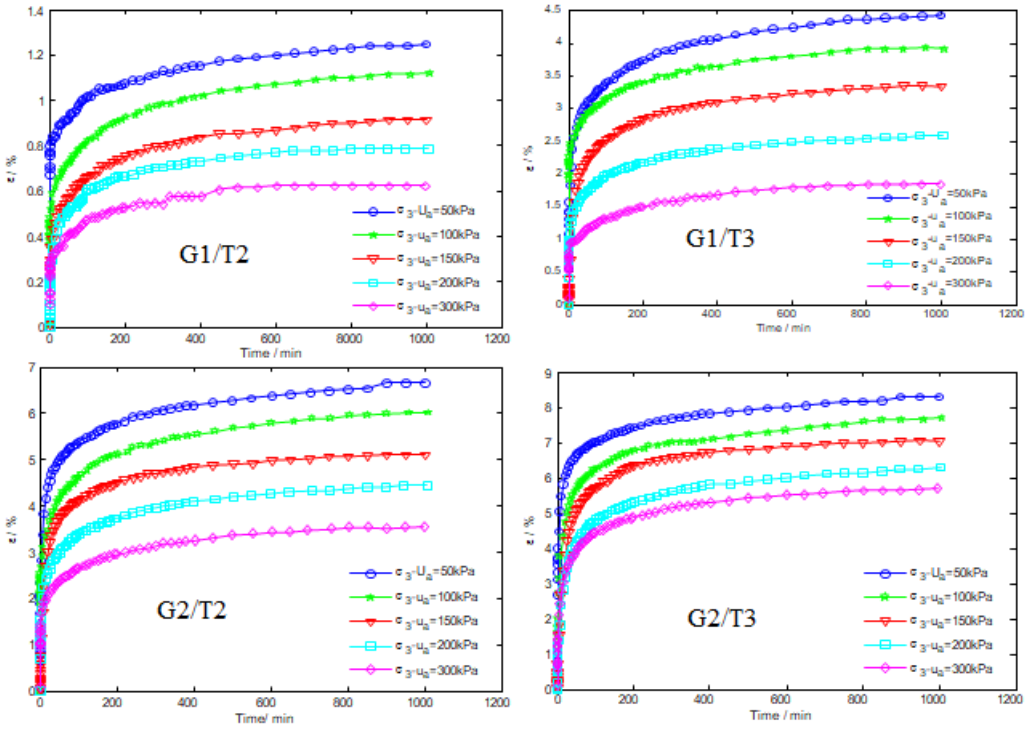

Figure 13. Creep test curve for controlling matric suction

The soil matrix of soils susceptible to suffusion is usually composed of mixed coarse and fine particles. Under certain geometric and hydro-mechanical conditions, the fine particles can be detached from the solid skeleton and behave as a part of the liquid phase in the form of liquidize fine particles, which can be transported away by the flowing liquid. The loss of fine particles in the soil of bank slope leads to the change in microstructure of the soil. The nonlinearity of the permeability coefficient is a typical characteristic of the soil subjected to seepage erosion on the micro scale. Base on the theory put forward by the relationship, three-dimensional creep model of unsaturated soil is established in accordance with the model test results. Three-dimensional creep model of unsaturated soil can be expressed as follows:

$$\left.\begin{aligned}
&\varepsilon_{ij}=\frac{S_{ij}''}{3K'}+\frac{2}{E_u/\tau_f}\cdot\frac{\bar{D}}{1-R_f\bar{D}}\left[\frac{1}{3G_H'}+\frac{1}{3\eta_1'}t+\frac{1}{3G_{l1}'}\left(1-e^{-G_{l1}'t/\eta_2'}\right)+\frac{1}{3G_{l2}'}\left(1-e^{-G_{l2}'t/\eta_3'}\right)\right]\\
&\bar{D}=\frac{S_{ij}'}{\tau_f}\ ,\quad \tau_f=c^{/}+\left(\sigma-u_a\right)\tan\phi^{/}+\left(u_a-u_w\right)\tan\phi^{b}\\
&K'=\frac{2(1+\mu)}{3(1-2\mu)}G_H'\ ,\ G_H'=a_{G_H}\sigma_3'+G_H^{\,0}\ ,G_{l1}'=a_{G_{l1}}\sigma_3'+G_{l1}^{\,0}\ ,\ G_{l2}'=a_{G_{l2}}\sigma_3'+G_{l2}^{\,0}\\
&\eta_1'=a_{\eta_1}\sigma_3'+\eta_1^{\,0}\ ,\quad \frac{G_{l1}'}{\eta_2'}=a_{G_{l1}/\eta_2}\sigma_3'+(\frac{G_{l1}}{\eta_2})^0,\frac{G_{l2}'}{\eta_3'}=a_{G_{l2}/\eta_3}\sigma_3'+(\frac{G_{l2}}{\eta_3})^0\\
&\sigma_3'=\sigma_3-s=\sigma_3-u_a
\end{aligned}\right\}\qquad(11)$$

Where: S''_{ij} is deviatoric stress tensor; S'_{ij} is the spherical stress tensor; E_u is the initial tangent modulus. τf is the shear strength. D is the normalized shear stress. K is the volume modulus.

$$K=2(1+\mu)\,G_H/[3(1-2\mu)]\qquad(12)$$

μ is Poisson's ratio; R_f is the failure ratio; G_H and η_1 are the shear modulus and viscosity coefficient of Maxwell body respectively; G_{l1},G_{l2} and η_2， η_3 are the shear modulus and viscosity coefficient of Kelvin body respectively; t is time; c' is effective cohesion; φ' is the effective internal friction angle; σ is stress; u_a is pore gas pressure; u_w is the pore water pressure; u_a-u_w is matric suction; φ^b is the internal friction Angle varying with matric suction.

This paper is study the rheological curves of different matric suction. We are investigated the effect of net confining pressure, a variable containing matric suction, on the rheology of unsaturated soil. We are research the characteristics of unsaturated creep curve. It is analog the modeling idea of saturated creep model. The net confining pressure is considered as a new stress variable. We are studied the relationship between net confining pressure and strain. So that matric suction is reflected in the creep model. The creep model of unsaturated soil can reflect the stress - strain - time - matric suction simultaneously.

The extended Berg creep model have contains a negative exponential term. The parameters are generally obtained by nonlinear least square regression method. However, it is the nonlinear least square regression method often produces different results, that is, there are multiple groups of different matches for the parameter. In this paper, the parameters of the established model have clear physical meanings. So, we can according to its physical significance and creep curve characteristics. We are find a set of initial values close to the actual values. Therefore, it is necessary to calculate unsaturated seepage at the same time when solving unsaturated creep model.

Calculation example of slope reliability

Slope model and its G-Line failure domain

We are taking a generalized model of a homogeneous slope as an example. The geometric shape of the slope is shown in Fig. 14.We were selected the shear strength parameters C and φ, which are most sensitive to reliability, as random variables. This example is mainly to illustrate the application of Copula function integral calculation of slope failure probability based on G-line failure domain. The variables c and φ are calculated according to Equations (3) and (4) in this paper, the mean values were 19.3kPa and 0.35, respectively. The corresponding

coefficients of variation were 0.3 and 0.15, respectively. In addition, the other slope shape parameters and bulk density with small variability are regarded as deterministic quantities. The slope height H=60.0m, the slope Angle β=45°, and the bulk density γ=18kN/m^3.

Multiple experts[53,56] have been established two random Gaussian, Frank, Clayton, Gumbet and Placket multiple Copula Joint distribution model. We are aiming at the reliability analysis of the slope. We are starting from the calculation of failure probability. We are base of the above five Copula and the slope G-line functions. We were used to Copula direct integration and Monte Carlo methods calculate the homogeneous failure probability.

The slope model is shown in Figure 14. We are given the G-line curve of the slope model and its quadratic polynomial fitting expression. The determination coefficient R2 was 0.9788. After calculation, the parameter range of cohesion C representing the failure region of the slope is obtained， that is $0<c<c_{max}$，

c_{max} =[-B-(B^2-4AC)$^{1/2}$]/2A=139.8kPa.

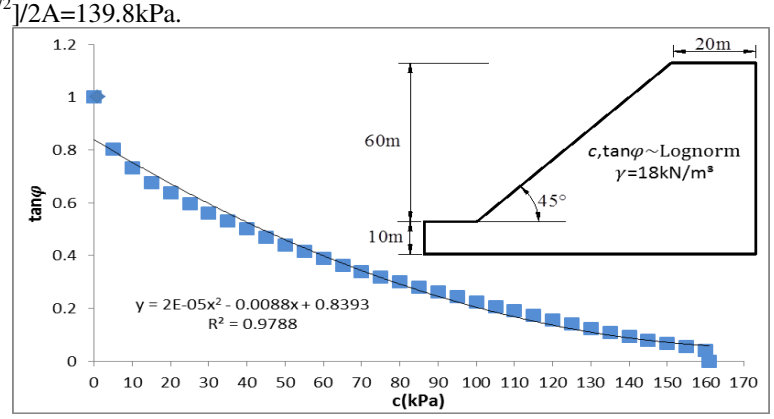

Figure.14 Geometry of the instanced slope and its g-line curve

Slope failure probability calculation

Copula can conveniently establish the joint distribution function with arbitrary edge distribution and related structural variables. Again, we are using the idea of the inverse transform. The joint distribution function established by Copula is used to realize the sampling of two-dimensional random variables C and tanφ. At this time, the obtained C and tanφ obey their respective edge distribution. It is also satisfies the specific correlation and joint distribution model. The two-dimensional Gaussian, Frank and Placket Copula functions have selected symmetry. We are facilitate the description of the negative correlation between parameters. With Frank copulas connect (θ = 4.1762) as an example. Figure 15 shows its probability density and distribution. The AIC and PC values of each Copula function are shown in Table 4.

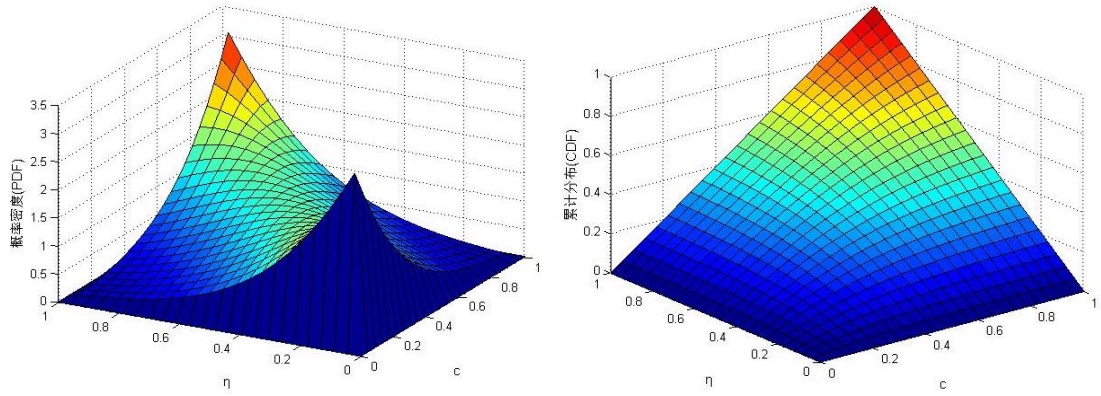

(**a**) Probability density function graph (**b**) Cumulative distribution function graph

Figure. 15 Graphs of density and distribution of Frank Copula function（θ=4.1762）

We are be seen from Table 4.In the Copula function, the Gaussian Copula has a smaller AIC value, while the Placket Copula has a larger pc value. The evaluation effect of Frank Copula is relatively poor among the three, indicating that there is not only one optimal Copula obtained by different evaluation approaches. Figure 16 are shows the use of the above copulas connect function structural shear strength parameters c and tan φ joint density function of the equivalent figure. It can be seen that the parameters described by various copulas are all negatively correlated. The Gaussian and Placket Copula isograms are close to each other and have good symmetry. On the other hand, Frank Copula has poor symmetry.

Copula	Gaussian	Frank	Clayton	Gumbel	Placket	Coefficient
Parameters	0.713	5.833	2.043	2.021	6.742	
AICc	-41.5624	-39.7236	-50.2413	-37.1446	-35.8777	ρ=0.582
Sn/pc	0.0691	0.0653	0.0428	0.0501	0.0660	τ=0.505
RMSE	0.1971	0.2001	0.1883	0.2007	0.2024	
Bias	17.5320	18.2187	16.3862	18.0401	18.3461	

Table 4. Values of the AICc, S_n/p_c, RMSE, Bias, correlation coefficient and copula parameter

Under the function represented by G-line curve, the corresponding failure probability was calculated using FORM and MCS methods. As shown in table 5. The error of the failure probability obtained by the integral method of Copula function relative to FORM and MCS method is also given in the table 5. The results obtained by Copula direct integration method are close to those obtained by the first-order reliability method (FORM) and Monte Carlo method (MCS). The maximum error in this example is only 5.58% of Placket Copula. We can establish the rationality of slope reliability analysis based on c-f joint probability density integral constructed by Copula function in G-line failure domain.

G/T	Gaussian	Frank	Clayton	Gumbel	Placket	MCS（g-line）
G1/T0	0.0496	0.0460	0.0582	0.0441	0.0413	0.0456
G1/T1	0.0176	0.0120	0.0239	0.0139	0.0114	0.0166
G1/T2	0.0533	0.0502	0.0621	0.0478	0.0450	0.0500
G1/T3	0.0216	0.0158	0.0284	0.0175	0.0148	0.0196
G2/T0	0.0161	0.0106	0.0221	0.0126	0.0201	0.0156
G2/T1	0.0880	0.0898	0.0961	0.0829	0.0801	0.0817
G2/T2	0.0420	0.0377	0.0503	0.0368	0.0341	0.0400
G2/T3	0.2613	0.2731	0.2547	0.2647	0.2577	0.2563

Table 5. Failure probabilities calculated by directly integration and MCS method

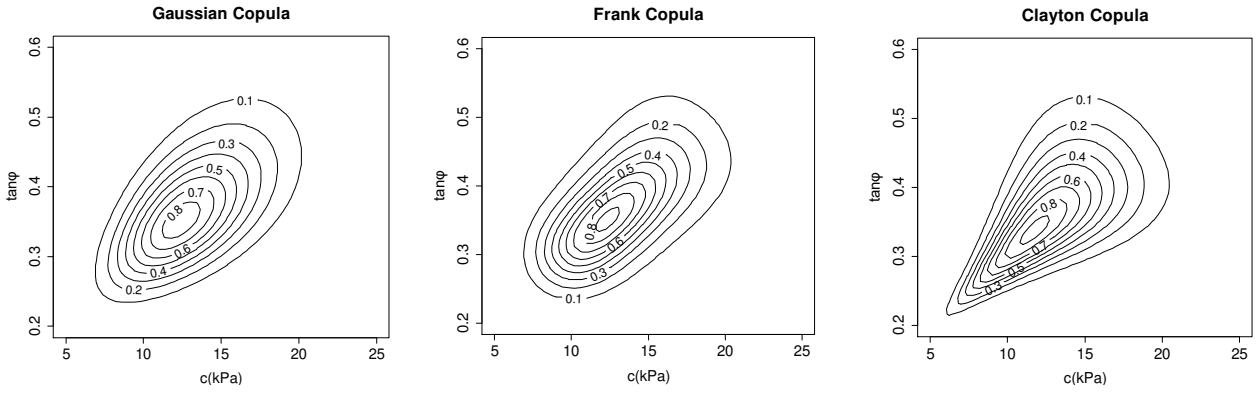

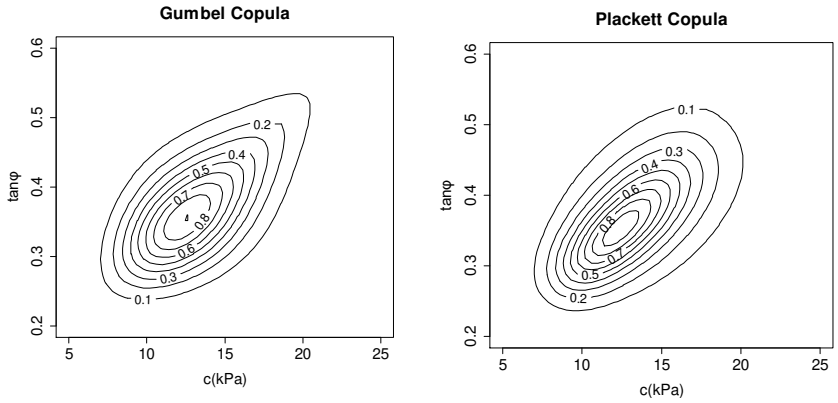

Figure.16 The joint density function with shear strength parameters associated in different Copulas

Results and discussion

We are further investigate the variation characteristics of slope failure probability difference with safety factor under different Copula functions. Table 6 is shows the slope safety factors of 6 groups with different mean values of c and f under the same coefficient of variation. At the same time, the table are also given the slope failure probability under different calculation methods and the ratio of the slope failure probability under Gaussian Copula function method.

G/T	Fs	Copula P_f / equivalent ratio			FROM P_f/ equivalent ratio	MCS P_f/ equivalent ratio
		Frank	Gaussian	Placket		
G1/T 0	1.667	3.0×10^{-4}/13	2.18×10^{-5}/1	4.94×10^{-4}/22.65		
G1/T1	1.617	0.00120/8	0.000 2/1	0.001 6/8	0.000 2/1.07	0.000 3/1.50
G1/T 2	1.533	0.0018/6	0.002 6/1	0.006 3/2.42	0.001 8/0.69	0.001 5/0.58
G1/T 3	1.216	0.005/2.08	0.007 8/1	0.017 3/2.22	0.011 7/1.50	0.011 2/1.44
G2/T1	1.516	0.012/1.64	0.069 7/1	0.067 4/0.97	0.057 6/0.83	0.057 4/0.82
G2/T 2	1.208	0.071/1.02	0.201 6/1	0.193 0/0.96	0.204 4/1.01	0.203 8/1.01
G2/T3	1.121	0.196/0.98	0.101 6/1	0.173 0/0.76	0.194 4/1	0.283 8/1

Table 6. Failure probabilities and equivalent rates of the slope calculated by different safety coefficients

Obviously, the failure probability of slope was decreases with the increase of safety factor. For Gaussian, Frank and Placket Copula functions, the corresponding failure probability is different. Combined with the equivalent ratio in Table 6, the difference of failure probability obtained by the three Copula functions under different safety factors has the following characteristics:

1) When the safety factor is large (F_s>1.4), the failure probability obtained by Placket Copula is relatively large, followed by Frank Copula and Gaussian Copula. At this point, the results of direct Placket Copula are relatively conservative. However, the results obtained by using Gaussian Copula directly overestimate the safety of the slope.

2) When the safety factor is small, the results obtained by the three copulas are close to each other. The difference is not significant. By the safety factor increases, the differences among the three are increasing rapidly. Such as the F_s=1.667, using the Frank and Placket copulas connect it is concluded that the failure probability of Gaussian results respectively 13.77 times and 22.65 times. It can be seen that when the probability of failure is low (the safety factor is high). The results of reliability analysis are sensitive to the type of Copula function.

3) The results obtained by conventional FORM and MCS method are close to those obtained by Gaussian Copula. The main reason is that the transformation of FORM method and the generation of random numbers in MCS method are still based on normal distribution in essence.

Different Copula functions have different structures, resulting in the difference of corresponding failure probability. As for the selection of the optimal Copula function, the results are not unique of different evaluation approaches. Therefore, it is particularly important to study the difference of slope failure probability under different Copula functions and the optimization of calculation results.

Conclusions

（1）We were established an ice-snow melting model based on physical process. In the process of ice-snow melting, the soil cohesion and internal friction Angle have obvious deterioration effect .The deterioration of cohesion is obviously larger than that of internal friction Angle. In the early part of the ice-snow melting cycle, the deterioration of shear strength parameters is very obvious. Among them, the deterioration of shear strength parameters caused by the first four ice-snow melting cycles accounted for about 70% of the total deterioration. After the G2/T2 ice-snow melting cycle, the degree of phase deterioration gradually decreases. The deterioration trend of shear parameters of soil samples gradually tends to be gentle.

(2) In the ice-snow melting cycle, the inside of the soil samples have micro-cracks, fissures repeatedly opened and closed, gradually developed and converged. The result is that the soil samples change from dense state to loose state where internal cracks develop. The internal damage of soil samples is the fundamental reason for the gradual deterioration of shear strength.

（3）We are keep to the relative independence principle of creep model and unsaturated seepage equation. We are studied and improved the parameter solving method of creep model. The modified model is reasonable and effective. The creep trend and main characteristics of the unsaturated soil can be described well.

(4) Different Copula functions have different structures, resulting in the difference of corresponding failure probability. As for the selection of the optimal Copula function, the results are not unique of different evaluation approaches. Therefore, it is particularly important to study the difference of slope failure probability under different Copula functions and the optimization of calculation results.

The soil deformation of landslide is the result of the combined action of seepage and creep. The seepage force generated by seepage will affect the creep characteristics of soil. The next step will focus on the coupling of creep and seepage.

Availability of data and material

The authors confirm that the data supporting the findings of this study are available within the article.

References

1. Yin, Y. P. Study on characteristics and disaster reduction of giant landslide on Bo mi Yi gong Expressway in Tibet. *Hydrogeology and geology engineering*.**04**, 8-11,DOI:https://doi.org/10.16030/j.cnki.issn.1000-3665.2000.04.003 (2000) (In Chinese with English abstract)
2. W. Liu, Study on the characteristics of huge scale-super high speed-long distance landslide Chain in Yi gong Tibet. *Journal of Geological Hazard and Control* .**13(3)**, 9-18 (2002). (In Chinese with English abstract)
3. Yin, K. L. Landslides in Switzerland and its research overview. *Journal of Geological Hazard and Control*. 10, 104-107(1999). (In Chinese with English abstract)
4. Xu , G.M. Study on mechanical properties of low-temperature, freeze-thaw damage and multi-field coupling of rock mass in cold zone. *Graduate school of Chinese academy of sciences.*2006.
5. Shamir, E., GeorGakakos , K. P. Distributed snow accumulation and ablation modeling in the American River basin. *Advances in Water Resources. 2*9,558-570. https://doi.org/10.1016/j.advwatres.2005.06.010（2006）
6. Singh. P., JAIN. S. K. Snow and glacier melt in the Satluj River at Bhakra Dam in the western Himalayan region. *Hydrological Sciences Journal*. , 47:1, 93-106, DOI: https://doi.org/10.1080/02626660209492910(2002)
7. Todd Walter, M., Brooks, E. S., Mcool, D .K. Process based snowmelt modeling: does it require more input data than temperature-index modeling. *Journal of Hydrology Amsterdam.***300**,65-75, DOI: https://doi.org/10.1016/j.jhydrol.2004.05.002(2005)
8. Fontaine, T. A., Cruickshank .T. S., Arnold. J. G. Development of a snowfall-snowmelt routine for mountainous terrain for the soil water assessment tool (SWAT). *Journal of Hydrology*.**262**,209-223, DOI: https://doi.org/10.1016/S0022-1694(02)00029-X(2002)

9. Ambrose. B., Freer. J.,Beven, K. Application of a generalized TOPMODEL to the small Ringelbach catchment，Vosges，France． *Water Resources Research.* **32**,2147-2159, DOI: https://doi.org/10.1029/95WR03715(1996)
10. Shaun Sellers. Theory of water transport in melting snow with a moving surface. *Cold Reg. Sci. Technol*. 31, 47-57. DOI: https://doi.org/10.1016/S0165-232X(00)00006-9(2000)
11. Shalamu Abudu, Sheng, Z. p., Cui, C.L. Integration of aspect and slope in snowmelt runoff modeling in a mountain watershed. *Water Science and Engineering*.**9(04)**,265-273,DOI: http://dx.doi.org/10.1016/j.wse.2016.07.002 (2016)
12. Zhang, Y.X., Song, X.C. ,Wang, G.L. Analysis of rock slope overturning stability under extreme ice and snow conditions. Journal of rock mechanics and engineering. 29,1164-1171, DOI: https://doi.org/1000–6915(2010)06–1164–08 (2010)
13. Qian , X.H., Rong, G., Huang, K. Seepage calculation and stability analysis of slope under melting snow infiltration. Journal of geological hazards and prevention.2010,21, 27-33. : DOI: https://doi.org/1003-8035(2010)04-0027-07 (2010)
14. Wei, X.L., Chen, B. C., Zhao, L., Zhao. N., Li. B. Kinematic characteristics and emergency response model of loess landslide were drive by snowmelt: take the Zeketai Landslide in Yi li ， Xinjiang as an example . *Journal of Geological Hazard and Control.* **31**,78-90,DOI: https://doi.org/10.16031/j.cnki.issn.1003-8035.2020.06.10 (2020)
15. Ge, Q. Study on soil slope stability in seasonal frozen area based on strength damage of freezing-thawing interface. *Jilin university.* 2010.
16. Xu，Q ., Liu, Z. H. ,Fang, S.F. Retrieval method for estimating snow depth using hyperspectral data in snowmelt period. *Spectroscopy and Spectral Analysis*.**33**, 1927-1931.(2013). (In Chinese with English abstract)
17. Huang， X . D., Zhang, X.T., Li ,X. Accuracy analysis for MODIS snow products of MODIOA1and MOD10A2 in northern Xinjiang Area. *Journal of Glaciology and Geocryology*.**29**, 722-729, DOI: https://doi.org/1000-0240(2007) 05-0722-08(2007) (In Chinese with English abstract)
18. Gao, T. G.Analysis and simulation of the hydrological processes in the Nam Co Basin, Tibet an Plateau. *Chinese Academy of Sciences*.2011. (In Chinese with English abstract)
19. Cao ,Y., Yin, K., Alexander, D. E., Zhou ,C. Using an extreme learning machine to predict the displacement of step like landslides in relation to controlling factors. *Landslides*. **13**, 725–736, DOI: https://doi.org/10.1007/s10346-015-0596-z(2016),
20. Liu SY, Wu TH, Wang X, et al., Changes in the global cryosphere and their impacts: A review and new perspective. *Sciences in Cold and Arid Regions*.**12(6)**,343−354,DOI: https://doi.org/ 10.3724/SP.J.1226.2020.00343 (2020).
21. The Professional Standards Compilation Group of People's Republic of China. SL237-1999 Specification of soil test. *Beijing: China Water Power Press*.(1999).
22. Zhang, G.S. A study of the Zhadang glacier energy and mass balance and its hydrological processes in Na m Co basin，central Tibetan Plateau. *Chinese Academy of Sciences*.(2013). (In Chinese with English abstract)
23. Guo，Z.M. ,Wang, N.L. Progress in the research on snow grain size retrieved from remote Sensing. *Journal of Glaciology and Geocryology* . **33**, 539-545. DOI: https://doi.org/1000-0240(2011)03-0539-07. (2011)
24. Chen, F., Cai, Q.G., Zheng, M.G., Sun, L.Y. Melting characteristics and ablation calculation in Nam Co basin. *Journal of Mountain Research*.**33**, 465-472,DOI：https://doi.org/10.16089/j.cnki.1008-2786.000058 (2015)
25. Xiong , L.S., Lin, C.J.， Xu, J.R. Application of energy balance snowmelt model on sunny slope in western Tianshan Mountains. *Agricultural Science and Technology*. **13**, 872-876, DOI：https://doi.org/10.16175/j.cnki.1009-4229.2012.04.022 (2012)
26. Miao ,H. B.; Yin，K. L.; Xing, L. X. ;Zhang, Z. Y. Evolution analysis of loose debris slope under condition of extreme snow hazard. *Rock and Soil mechanics*.**33**, 147-153+161,DOI：https://doi.org/10.16285/j.rsm.2012.01.016 (2012)
27. Xiong, T.Q., Li, J. L. ,Wang ,L.H. , Deng ,H.F., Xu , X.L. Reservoir Landslide Physical Modeling under Ice-Snow Melting and Reservoir Water Combined Action. *Advances in Civil Engineering*.**12**,1-21. DOI: https://doi.org/10.1155/2020/8832485(2020)
28. Le, T. M. H., Gallipoli, D., Sánchez, M. Stability and failure mass of unsaturated heterogeneous slopes. *Canadian Geotechnical Journal*.**52**, 1747-1761. DOI: https://doi.org/10.1139/cgj-2014-0190（2015）
29. Wang, D. J., Tang ,H. M., Zhang, Y. H. An improved approach for evaluating the time-dependent stability of colluvial landslides during intense rainfall. *Environmental Earth Sciences*. 76,321-336. DOI: https://doi.org/10.1007/s12665-017-6639-0(2017)
30. Le ,T .M. H.， Gallipoli , D.; Sánchez .M. Stability and failure mass of unsaturated heterogeneous slopes. *Canadian Geotechnical Journal.* **52**,1747-1761. DOI: https://doi.org/10.1139/cgj-2014-0190(2015)

31. Zizioli, D., Meisina, C., Valentino, R. Comparison between different approaches to modeling shallow landslide susceptibility: a case history in Oltrepo Pavese, Northern Italy. *Natural Hazards and Earth System Sciences.* 13,559-575, DOI: https://doi.org/10.5194/nhess-13-559-2013 (2013)
32. Tan,R. J.;Jiao, Y. J.;Xu, W. J. Tests on the creep parameters of the soft soil in Tianjin coastal region and analysis on the effect of subgrade settlement deformation . *Hydrogeology &Engineering Geology*. 42,67 -73. DOI：https://doi.org/10.16030/j.cnki.issn.1000-3665.2015.04.12(2015)
33. Xiong, Y. L.; Zhu, H .H.; Ye, G.L. Analysis of failure of unsaturated soil slope due to rainfall based on soil-water-air seepage-deformation coupling FEM. *Rock and Soil Mechanics.* 38,284-290, DOI：https://doi.org/10.16285/j.rsm.2017 .01.036 (2017)
34. Gao, J., Liao, M. K., Chang, D. Sensitivity analysis of the factors affecting the volumetric deformation of frozen sandy soil. *Journal of Glaciology and Geocryology.* **40** ,346-354,DOI：https://doi.org/1000-0240(2018) 02-0346-09 (2018)
35. Li ,X. L., Wang, H. J., Niu,Y. H. Strength and failure properties of frozen clay under varying loading rates. *Journal of Geotechnical Engineering*. **39** ,2335 -2340,DOI：https://doi.org/10.11779/CJGE201712024(2017)
36. Zhu, Y.B., Yu, H. M . An improved Mesri creep model for unsaturated weak intercalated soils. *Journal of Central South University*.**21**, 4677 – 4681,DOI: https://doi.org/10.1007/s11771-014-2476-4（2014）
37. Sun. M. J., Tang, H. M., Wang, X. H. Creep properties of sliding-zone soil from a creeping landslide. Rock and Soil Mechanics，，38, 385-391. DOI: https://doi.org/10.16285/j.rsm.2017.02.011(2017)
38. Zou, L.C., Wang, S.M., Lai, X.L. Creep Model for Unsaturated Soils in Sliding Zone of Qianjiang-ping Landslide. *Journal of Rock Mechanics and Geotechnical Engineering*. **5**, 162-167, DOI: https://doi.org/10.1016/j.jrmge.2013.03.001(2013)
39. Dang, J.Q., Zhang, B.P., Li, J. Uniaxial tension crack characteristics of loess. *Journal of Hydroelectric Engineering*. 26, 44－48(2001). (In Chinese with English abstract)
40. Deng, H.F., Yuan, X.F., Li, J. l. Research on failure characteristics and determination method for shear strength of earth-rock aggregate in direct shear tests. *Journal of Rock Mechanics and Engineering*.**32(Supp.2)**, 4065－4072,DOI：https://doi.org/10.16285/j.rsm.2014.04.005(2013)
41. Li, W.S., Wu, A. Q., Ding, X. l. Study on influencing factors of shear strength parameters of slide zone clay in Three Gorges reservoir area. *Rock and Soil Mechanics.* **27**, 56－60, DOI：https://doi.org/10.16285/j.rsm.2006.01.011（2006）
42. G. Siemens, S. B. Peters, W. A. Take. Characterization of Transparent Soil for Unsaturated Applications. **34(5)**,445-456, DOI: https://doi.org/10.1520/GTJ1035809 2011）
43. KONDO. J.， YAMAZAKI. T. A prediction model for snowmelt ，snow surface temperature and freezing depth using a heat balance method . *Journal of Applied Meteorology*.**29**, 375-384(1990).
44. SHAMIR, E.,GEORGAKAKOS. K. P. Distributed snow accumulation and ablation modeling in the American River basin. *Advances in Water Resources*.**29**,558-570, DOI: https://doi.org/10.1016/j.advwatres.2005.06.010(2006)
45. Kaye, Brubaker. Snow and Glacier Hydrology. *EOS, TRANSACTIONS AMERICAN GEOPHYSICAL UNION*.**82(49)**,611-611. DOI: https://doi.org/10.1029/01EO00355(2001)
46. TODD ,WALTER. M., BROOKS, E .S, MCC OOL .D .K. Process-based snowmelt modeling: does it require more input data than temperature index modeling. *Journal of Hydrology*.**300**，65-75, DOI: https://doi.org/10.1016/j.jhydrol.2004.05.0029（2004）
47. Zhou, F., Qin ,S. Simulation of snowmelt runoff in JinGou River Basin based on SRM model . *Journal of China Institute of Water Resources and Hydropower Research* **.18(05)**,395-400, DOI: https://doi.org/10.13244/j.cnki.jiwhr.20200510 (2020)
48. FONTAINE, T, A., CRUICKSHANK, T .S.,ARNOLD ,J .G. Development of a snowfall-snowmelt routine for mountainous terrain for the soil water assessment tool . *Journal of Hydrology*.**262**,209-223,DOI: https://doi.org/10.1016/S0022-1694(02)00029-X(2002)
49. Li, D. Q, Tang ,X .S, Zhou, C. B, Phoon ,K .K. Uncertainty analysis of correlated non-normal geotechnical parameters using Gaussian copula. *Science China Technological Sciences*. **55(11)**,3081-3089, DOI: https://doi.org/10.1007/s11431-012-4937-z(2012)
50. Li, D. Q, Tang, X. S, Phoon ,K. K. Bivariate simulation using copula and its application to probabilistic pile settlement analysis. *International Journal for Numerical and Analytical Methods in Geomechanics*. **37(6)**,597-617,DOI: https://doi.org/10.1002/nag.1112(2013)

51. Tang, X .S, Li ,D. Q, Zhou, C. B, Zhang ,L. M. Bivariate distribution models using copulas for reliability analysis. *Proceedings of the Institution of Mechanical Engineers Part O: Journal of Risk and Reliability*.**227(5)**,499-512,DOI: https://doi.org/10.1177/1748006X13481928, (2013)
52. Tang, X .S., Li, D. Q., Rong, G., Phoon .K. K., Zhou, C. B. Impact of copula selection on geotechnical reliability under incomplete probability information. Computers and Geotechnics.49,264-278,
53. DOI: https://doi.org/10.1016/ j.compgeo.2012.12.002 (2013)
54. Tang ,X .S., Li, D .Q., Zhou, C. B, Phoon , K. K . Copula-based approaches for evaluating slope reliability under incomplete probability information. *Structural Safety*.**52**,90-99, DOI: https://doi.org/10.1016/j.strusafe.2014.09.007(2015)
55. Huang, D., Yang, C., Zeng, B. A copula-based method for estimating shear strength parameters of rock mass. Mathematical Problems in Engineering.**2014**,1-11,DOI: https://doi.org/10.1155/2014/693062(2014)
56. Manouchehr. Motamedi, Robert .Y. Liang. Probabilistic landslide hazard assessment using Copula modeling technique. *Landslides*. **11(4)**,565-573. DOI: https://doi.org/10.1007/s10346-013-0399-z(2014)
57. B.P. Marchant, N.P.A. Saby, C.C. Jolivet. Spatial prediction of soil properties with copulas. *Geoderma*. **162(3-4)**,327-34, DOI: https://doi.org/10.1016/j.geoderma.2011.03.005(2011)

Acknowledgments

This research is supported by the National Nature Science Foundation of China Grant, No. 51679127, No.51439003; National Natural Science Foundation of China Youth Fund Project, No. 51809151; Natural Science Foundation of Hubei Province, No. Z2018063; and Sponsored by Research Fund for Excellent Dissertation of China Three Gorges University, No. 2018BSPY004.

Author contributions statement

J.L.L. and H.F.D. conceived the research. T.Q.X. conceived the algorithm. T.Q.X. and X.L.X. conceived writing—original draft preparation. T.Q.X. and L.H.W. conceived writing—review and editing. J.L.L. conceived the funding acquisition. All authors have read and agreed to the published version of the manuscript.

Code availability

The software Copula was used to process and calculate the images in this study, and no custom code was used in this study.

Competing interests

The authors declare that they have no known competing financial interests or personal relationships that could have appeared to influence the work reported in this paper.

Figures

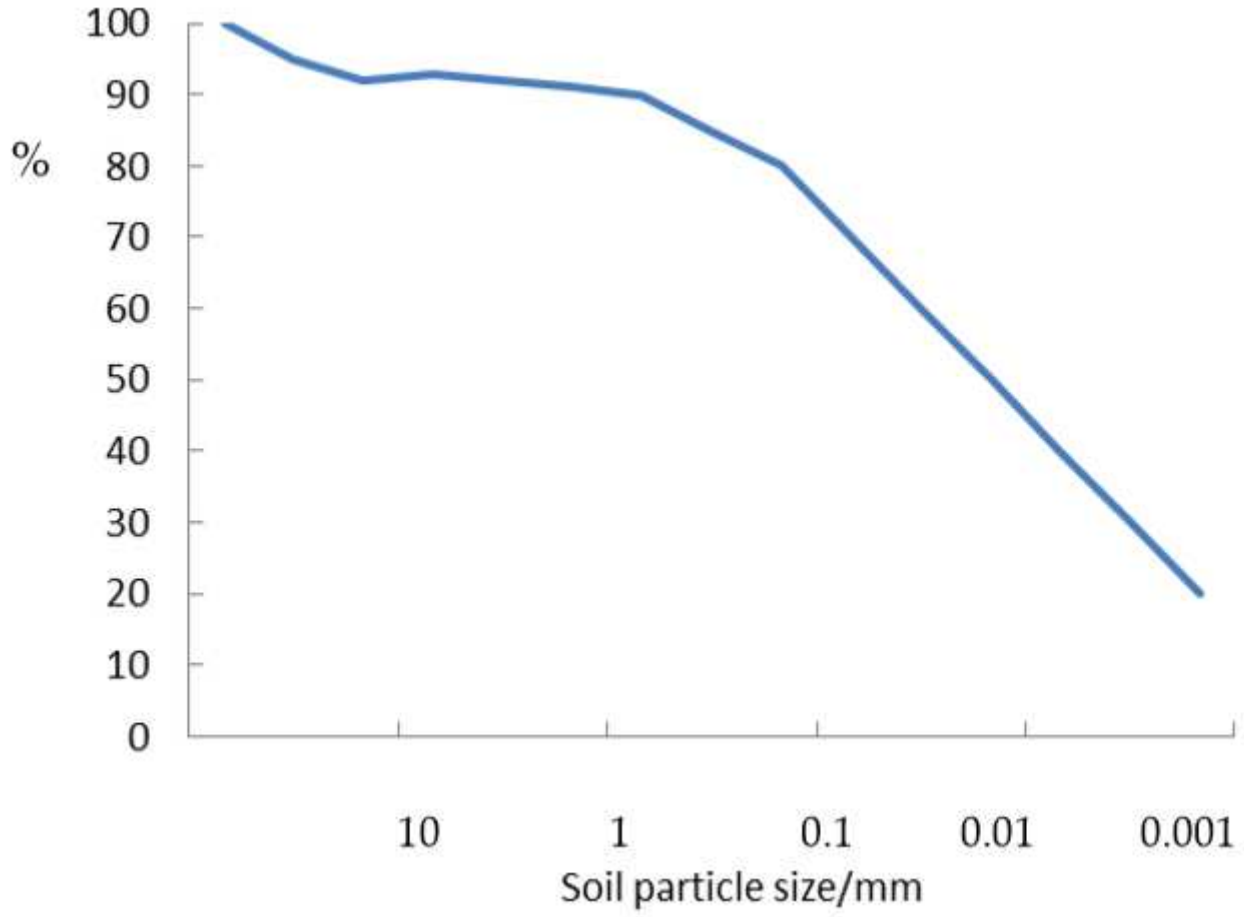

Figure 1

Grading curves of soil sample 111

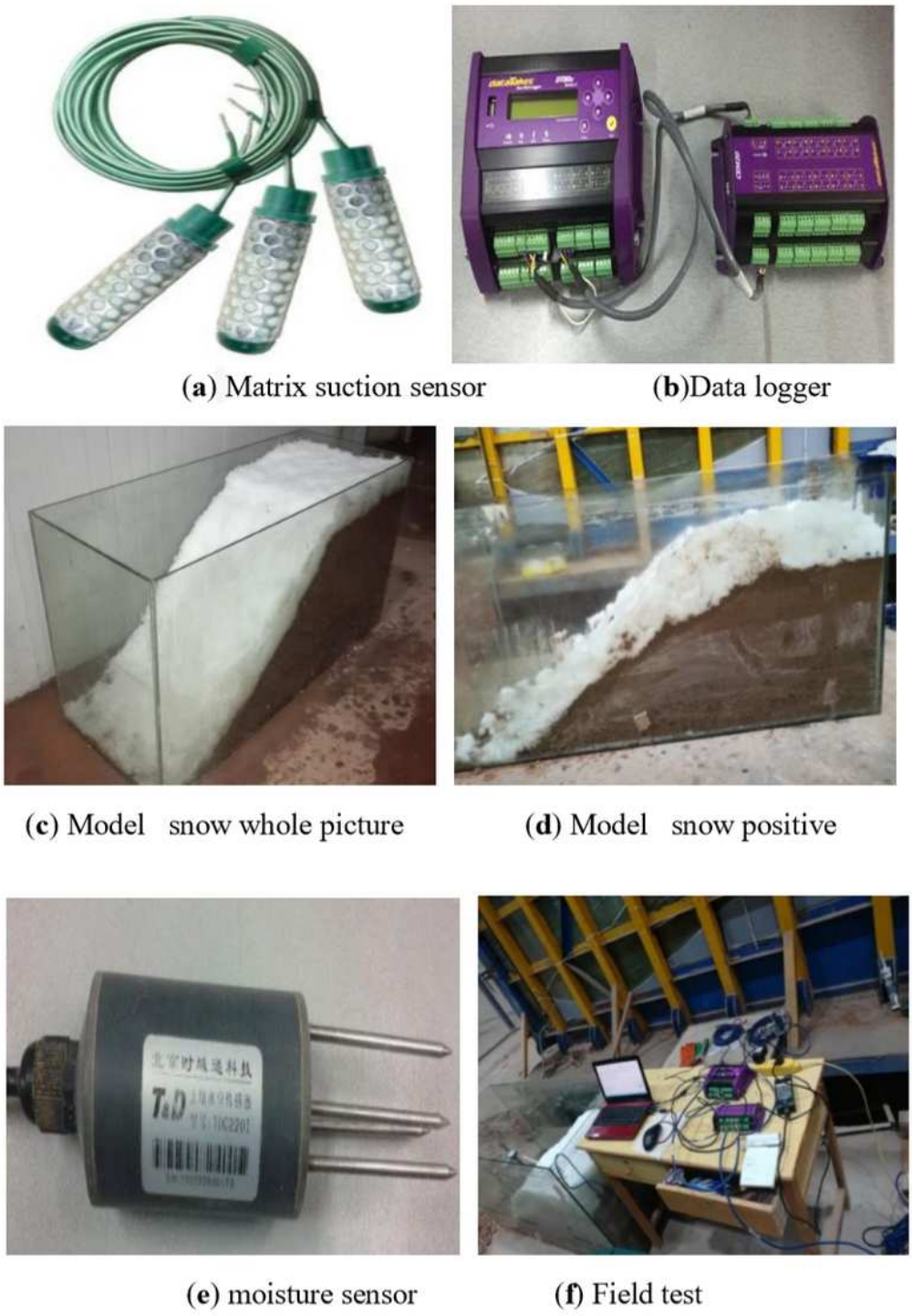

Figure 2

Multi-stage model test of ice-snow melting

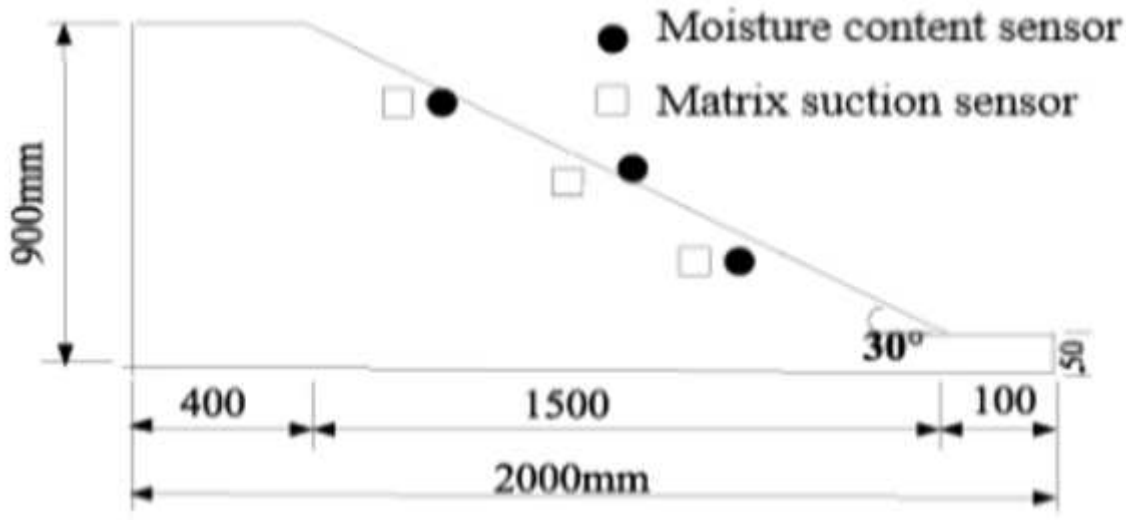

Figure 3

Sensor layout (take 30o slope foot as an example)

Figure 4

Direct shear test of soil samples

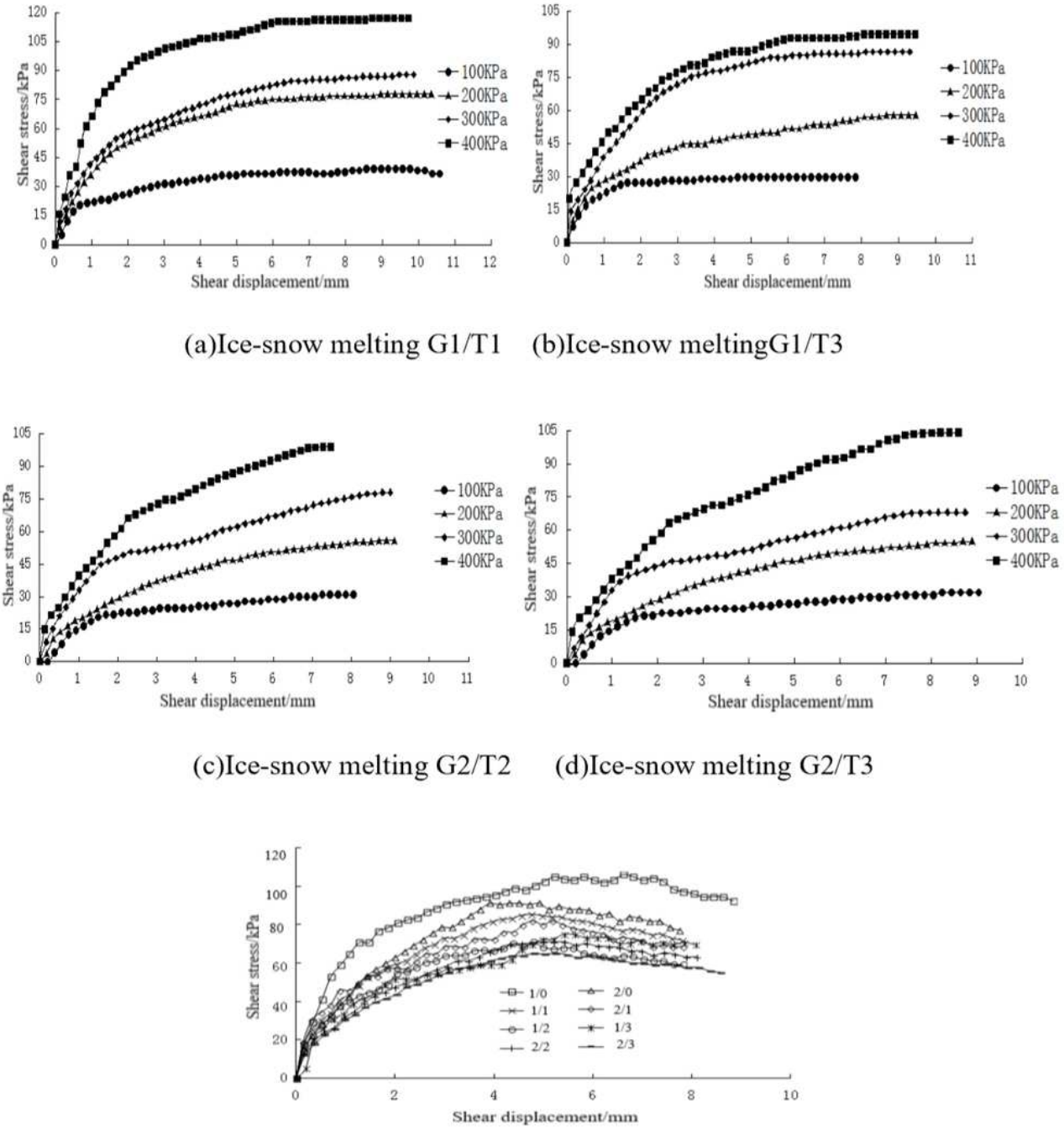

Figure 5

Ice-snow melting shear stress and shear displacement curve

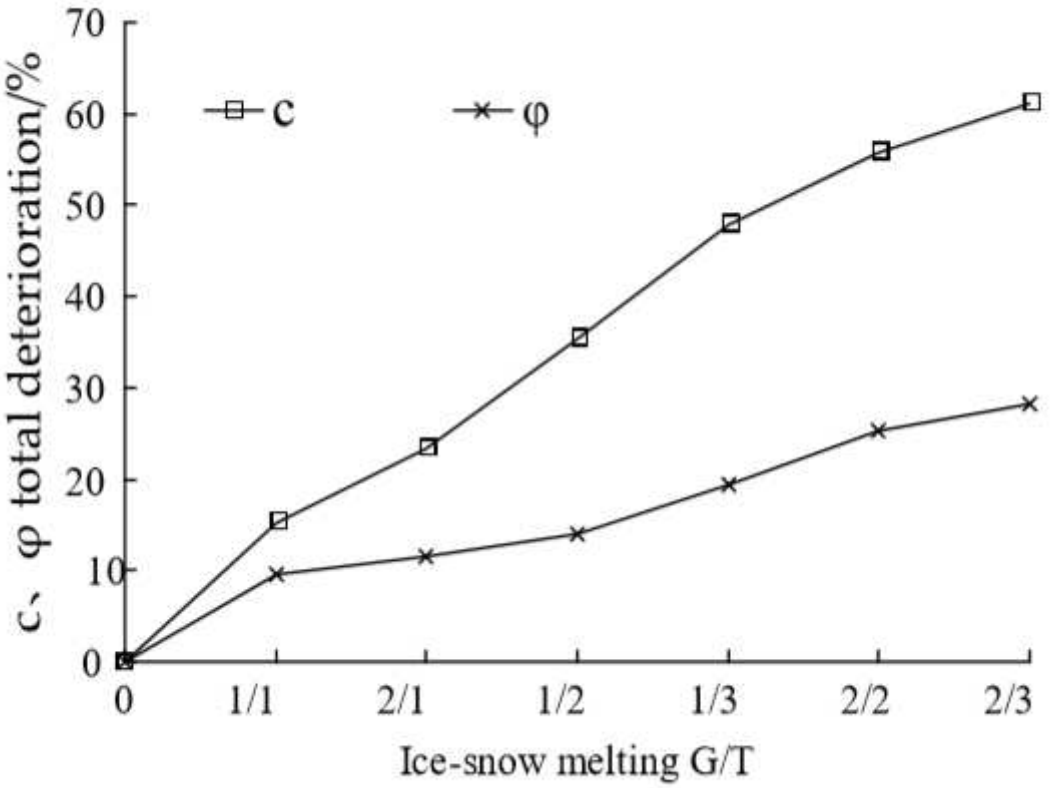

Figure 6

Total deterioration degree curves of cohesive force and internal friction angle

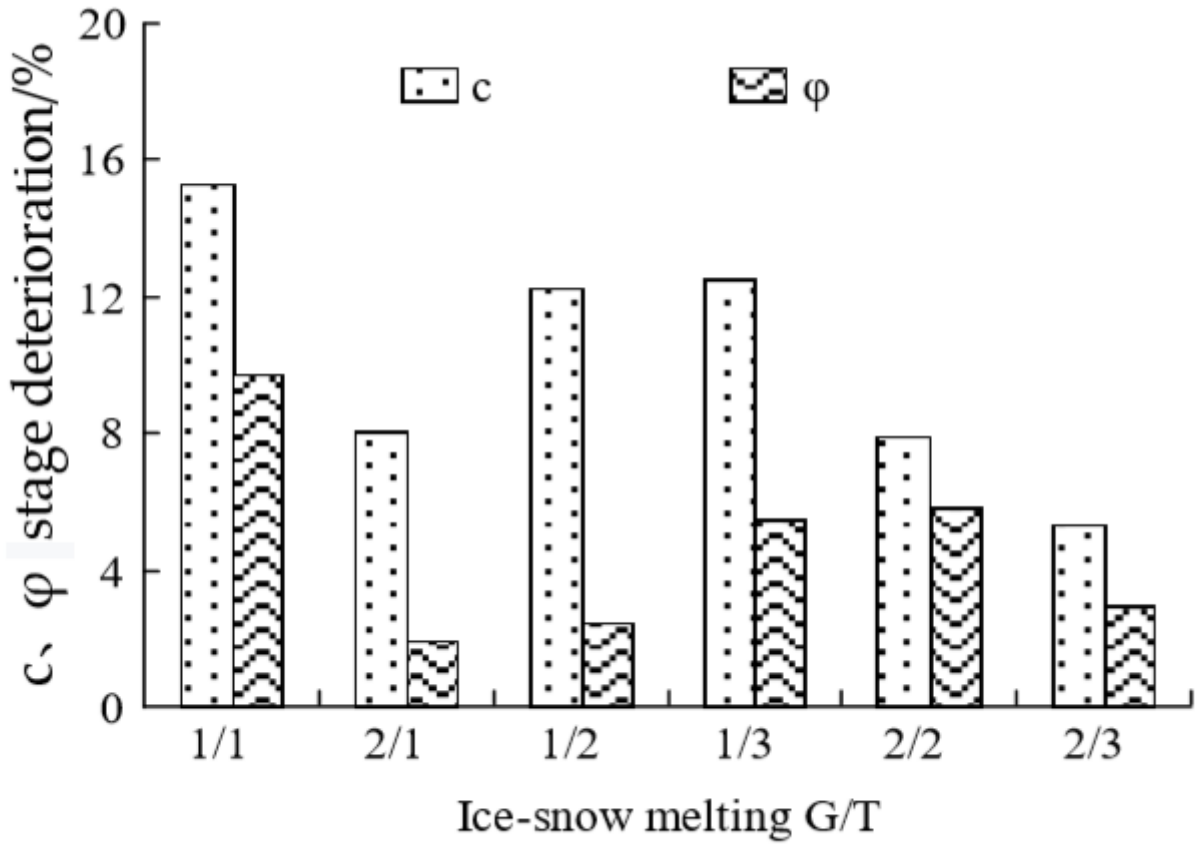

Figure 7

Stage deterioration degree curves of cohesive force and internal friction angle

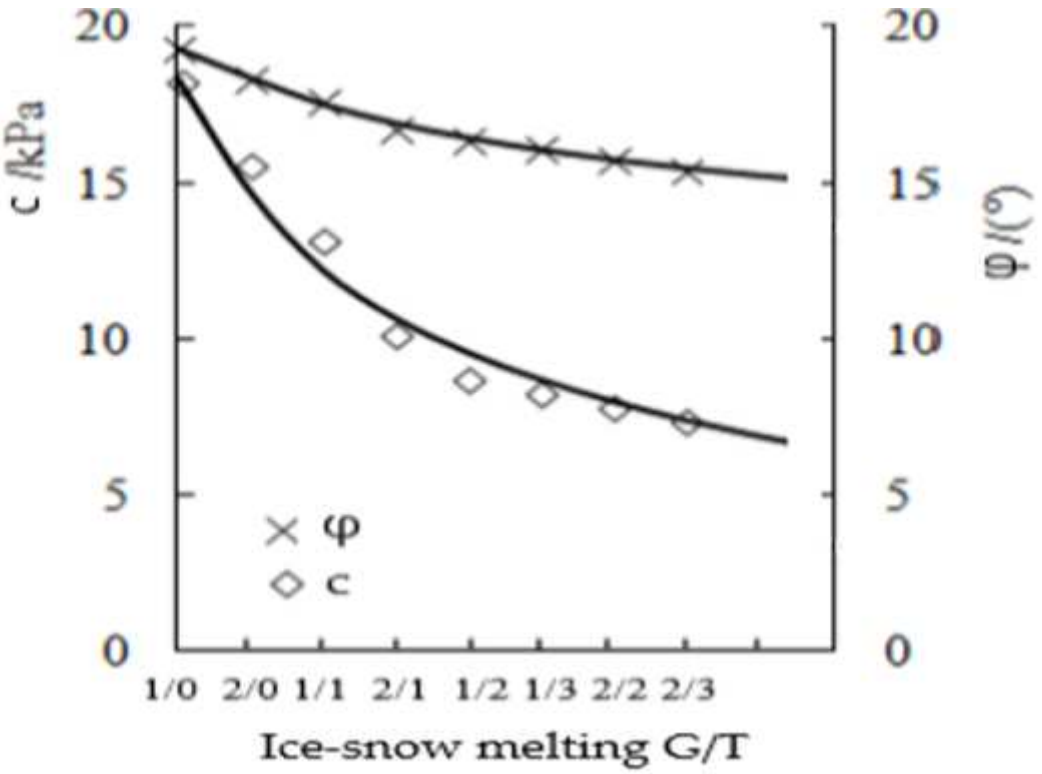

Figure 8

Deterioration rules of cohesive force and internal friction angle in ice-snow melting

Figure 9

Crack growth of sample surface

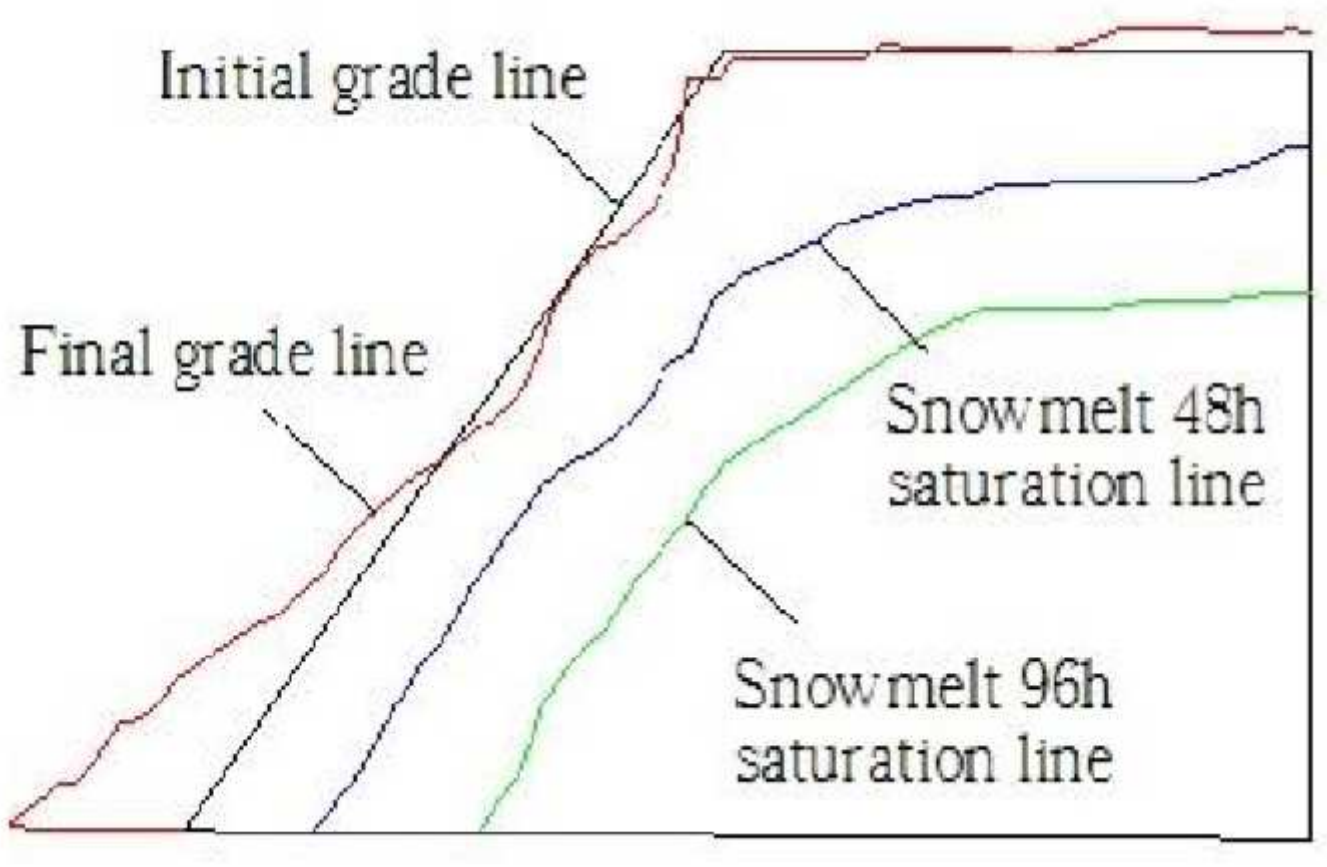

Figure 10

Infiltration line of snow water

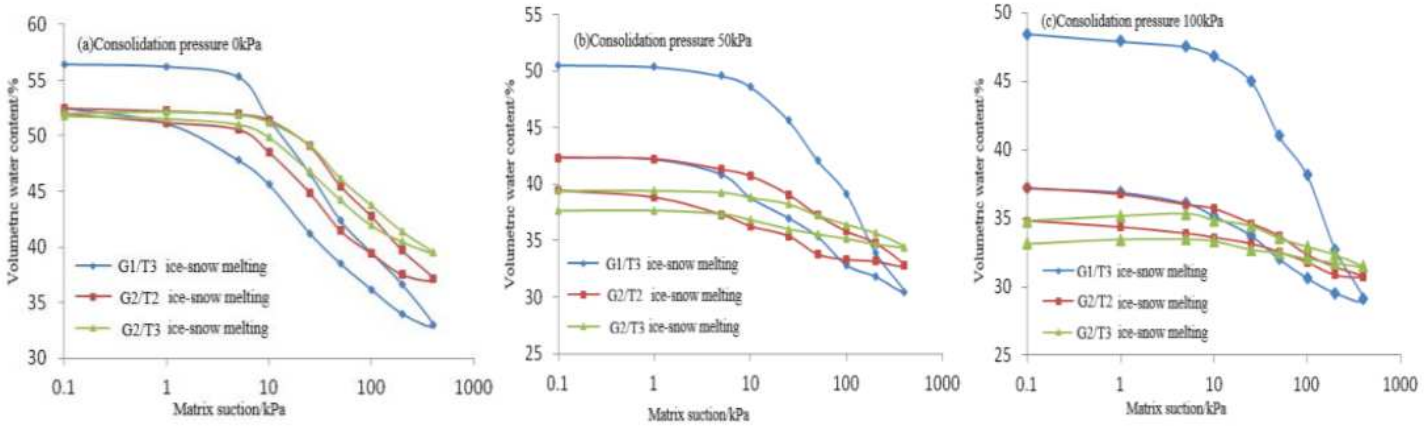

Figure 11

Relationship between water holding capacity and compressibility

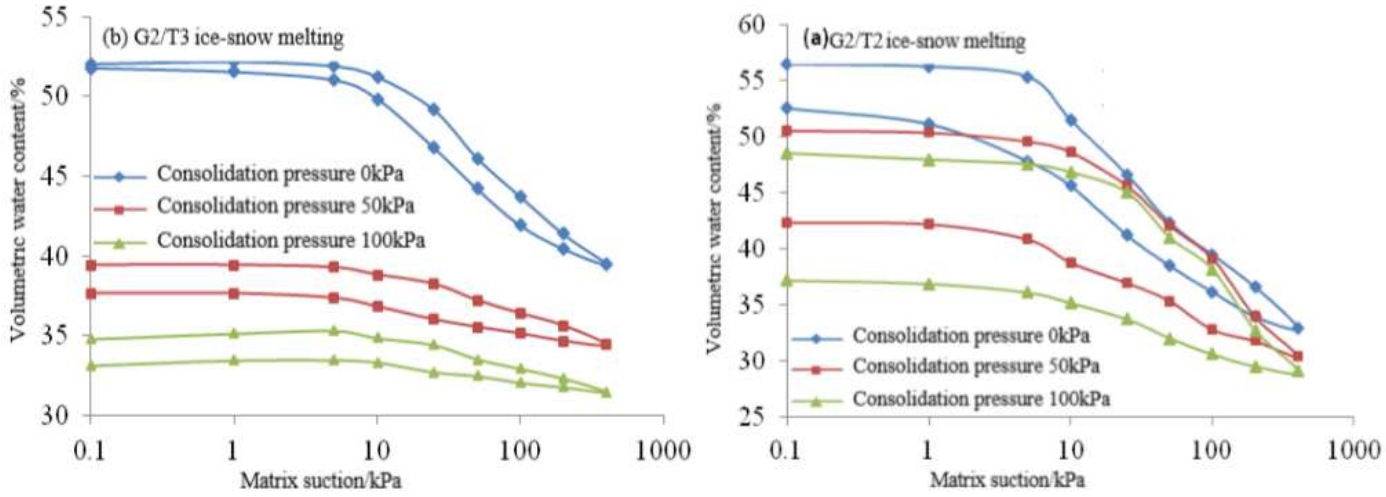

Figure 12

Effect of soil moisture and water holding capacity

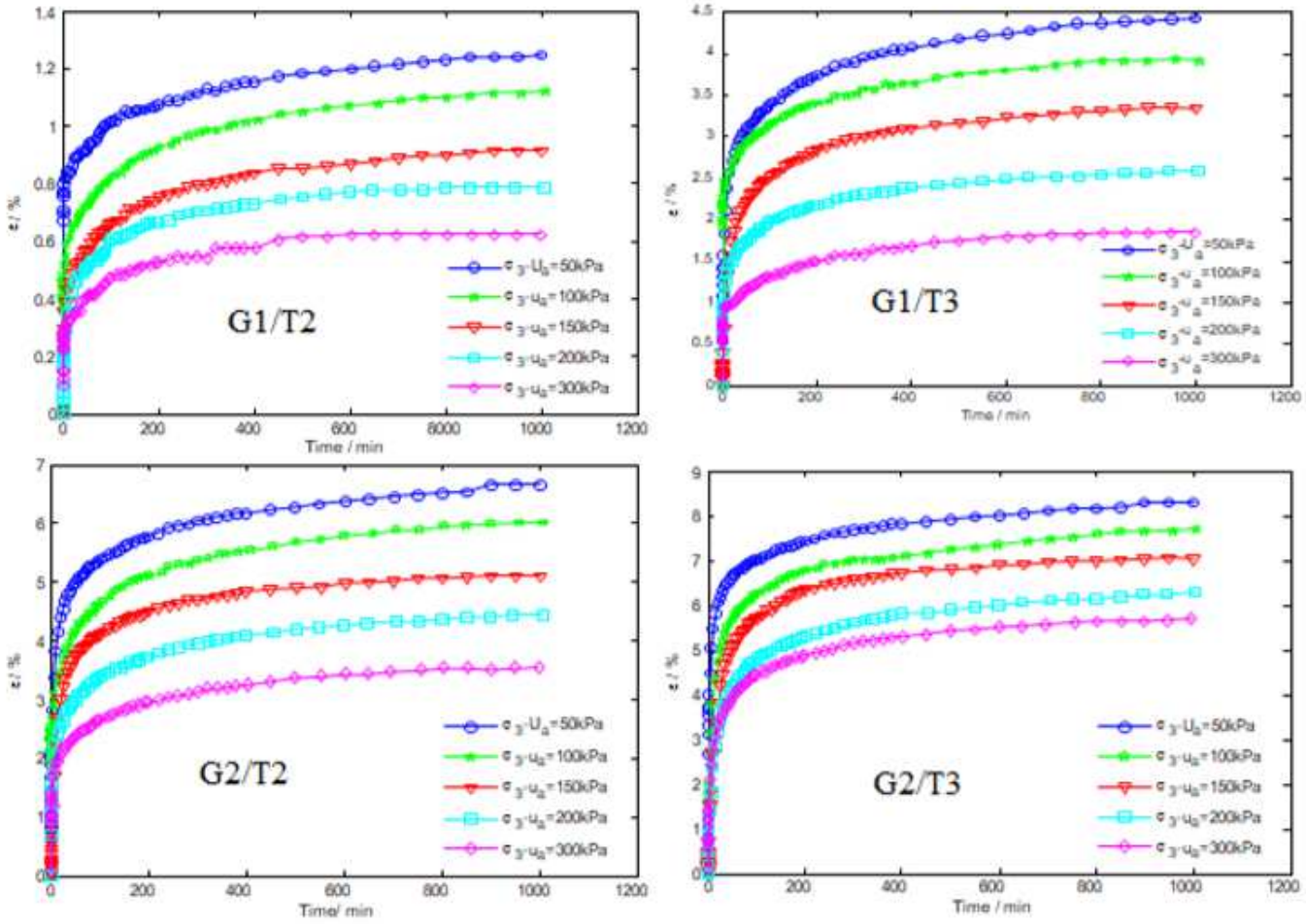

Figure 13

Creep test curve for controlling matric suction

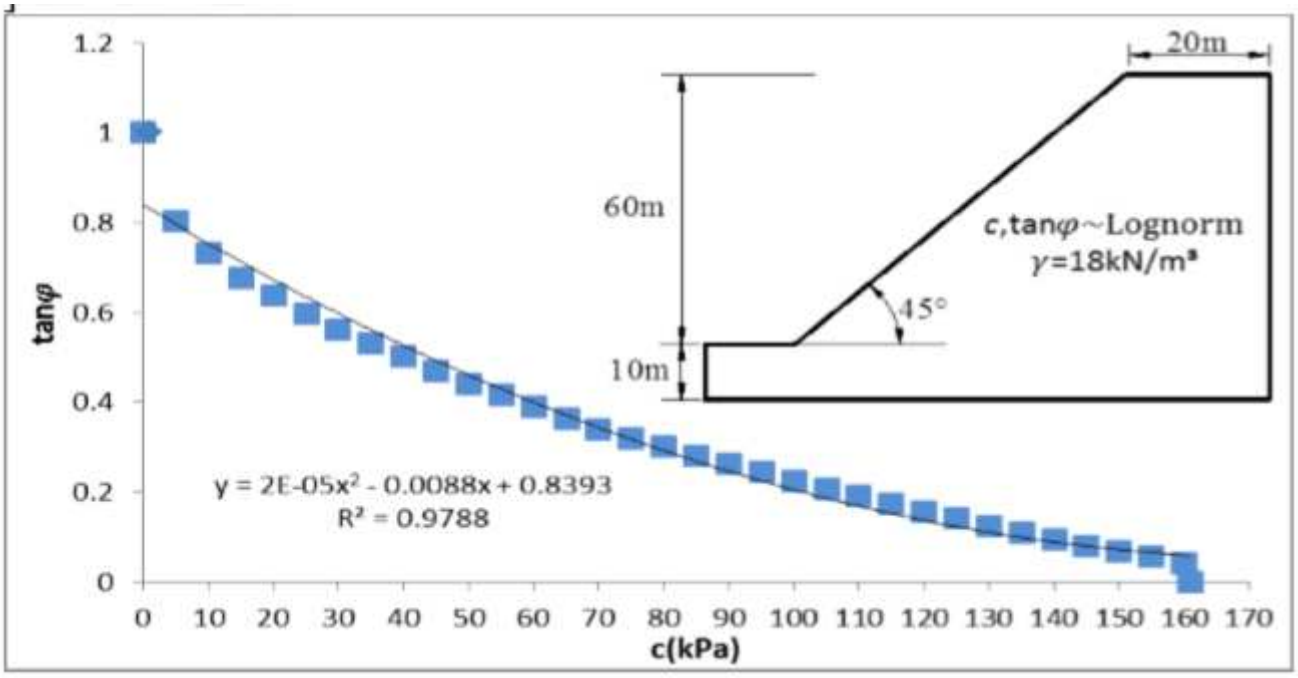

Figure 14

Geometry of the instanced slope and its g-line curve

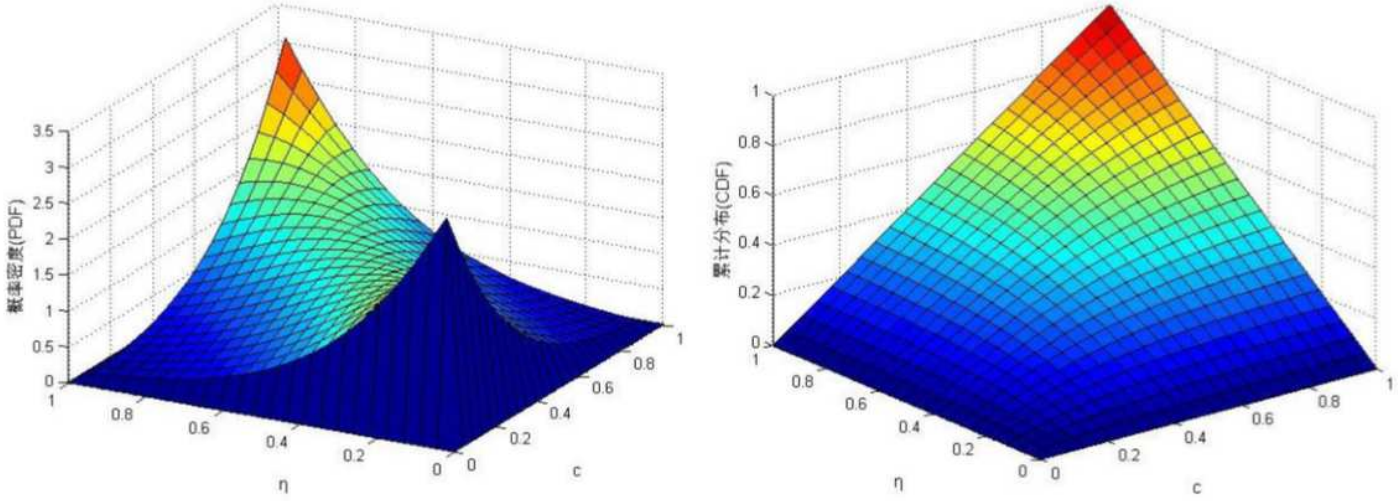

(**a**) Probability density function graph (**b**) Cumulative distribution function graph

Figure 15

Graphs of density and distribution of Frank Copula function□□=4.1762□

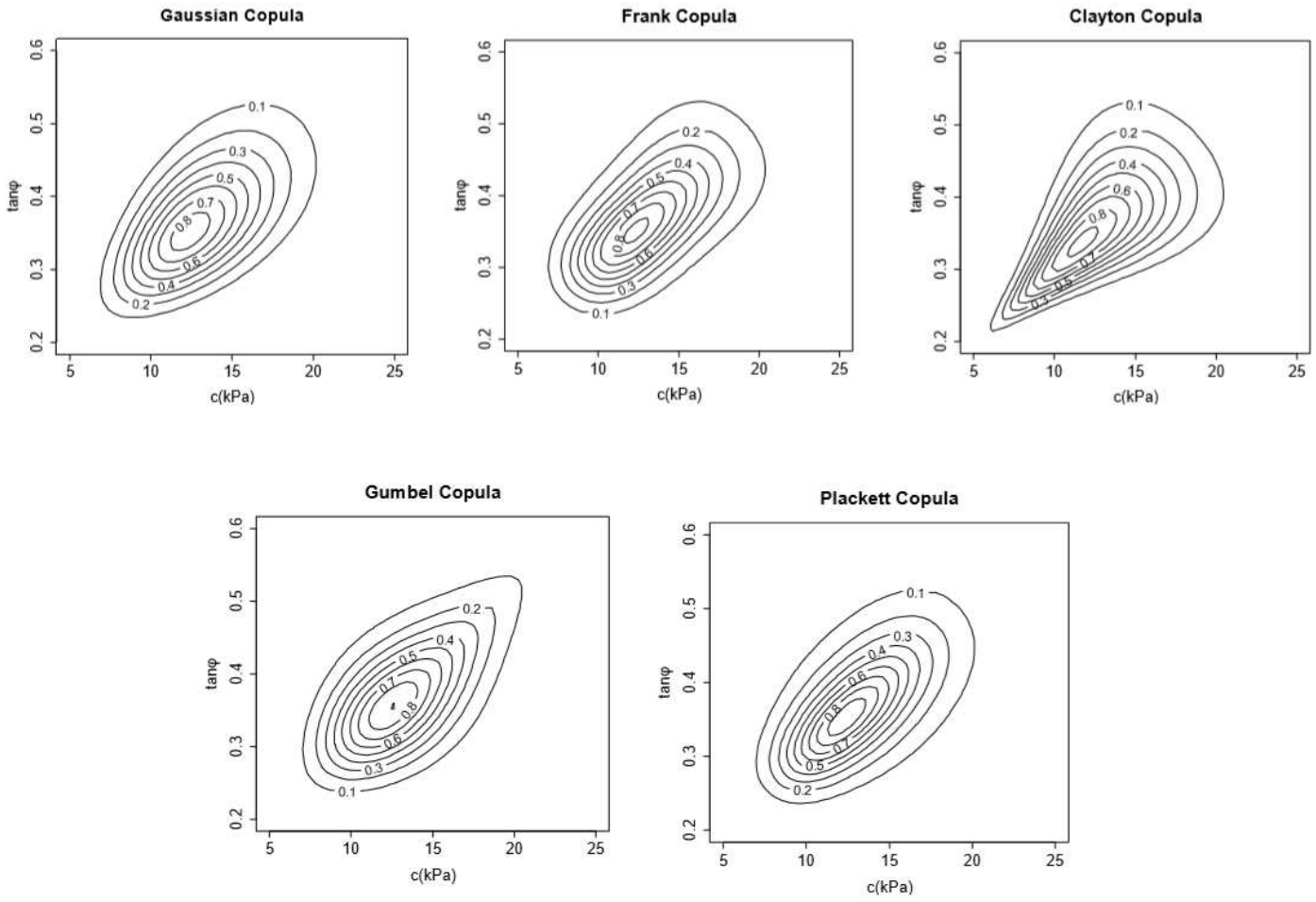

Figure 16

The joint density function with shear strength parameters associated in different Copulas